ISSN 2096-7071 (Print)
ISSN 2096-3101 (Online)
CN 10-1629/R1

CHINA CDC WEEKLY

Vol. 6 No. 13 Mar. 29, 2024

中国疾病预防控制中心周报

ENVIRONMENTAL HEALTH ISSUE

Preplanned Studies

Vital Surveillances

ISSN 2096-7071
9 772096 707248 13>

China CDC Weekly

Cover Image: adapted from the World Health Organization, https://www.paho.org/en/documents/infographics-how-environment-impacts-our-health.

Preplanned Studies

Acute Effects of Exposure to Fine Particulate Matter and Its Constituents on Sex Hormone Among Postmenopausal Women — Beijing, Tianjin, and Hebei PLADs, China, 2018–2019

Yanlin Tian[1,2,&]; Jiaonan Wang[3,&]; Jianlong Fang[3]; Chen Chen[3]; Feng Zhao[3]; Yi Zhang[3]; Peng Du[3]; Yawei Li[3]; Wanying Shi[3,4]; Yuanyuan Liu[3]; Enmin Ding[3]; Song Tang[3]; Xu Yue[2]; Xiaoming Shi[3,5,#]

Summary

What is already known on this topic?

Exposure to fine particulate matter ($PM_{2.5}$) was linked to endocrine hormone disruption in the reproductive system. Nonetheless, it was unclear which specific components of $PM_{2.5}$ were primarily responsible for these associations.

What is added by this report?

The study presented the initial epidemiological evidence that brief exposure to $PM_{2.5}$ can elevate estradiol levels in postmenopausal women. Various particle components had unique effects, with water-soluble ions and specific inorganic elements like Ag, As, Cd, Hg, Ni, Sb, Se, Sn, and Tl potentially playing significant roles in increasing estradiol levels.

What are the implications for public health practice?

The study established that the prevalence of air pollution, along with its specific components, has been recognized as a novel risk factor affecting the balance of sex hormones.

Recent studies have identified exposure to fine particulate matter ($PM_{2.5}$) as a potential risk factor for a range of adverse health outcomes (*1*–*3*). However, investigations into the relationship between $PM_{2.5}$ constituents and sex hormone levels have predominantly focused on men or women of reproductive age (*4*–*5*), leaving a gap in our understanding concerning postmenopausal women. Given that $PM_{2.5}$ can act as a xenobiotic influencing reproductive hormones, it is crucial to investigate its role in disease incidence among this demographic. Thus, our cross-sectional study sought to evaluate the correlations between short-term exposure to $PM_{2.5}$ and its components with sex hormone levels in postmenopausal women. This analysis utilized data from the Sub-Clinical Outcomes of Polluted Air in China. Additionally, we aimed to pinpoint the primary elements within the constituents in the Beijing-Tianjin-Hebei (BTH) region and adjacent areas (*6*). Our results indicate that $PM_{2.5}$ exposure is associated with a delayed increase in sex hormone levels, notably estradiol. Additionally, specific constituents of $PM_{2.5}$, particularly inorganic elements such as Ag, As, Cd, Hg, Ni, Sb, Se, Sn, Tl, and V, appear to be key contributors to elevated estradiol levels. The identification of air pollution and its distinct constituents as a novel risk factor for sex hormone equilibrium highlights the necessity of prioritizing interventions to mitigate its adverse effects on postmenopausal women.

In total, 1,033 women aged 40 years and older were recruited for the study, with participants stratified across age groups (40–49, 50–59, 60–69, 70–79, and 80–89 years) from the BTH region and adjacent areas using a stratified random sampling method between October 2018 and March 2019. This region, comprising nine cities, is known for high levels of air pollution and was selected for its advanced atmospheric monitoring infrastructure. Hourly data on ambient $PM_{2.5}$ levels and its components were sourced from the Chinese National Ambient Air Quality Monitoring Network. The exposure of participants to ambient $PM_{2.5}$ and its constituents was estimated using data from the monitoring stations within 2 km of their residences. We calculated the cumulative average exposure across different lag periods using these hourly data. After excluding 196 women who had not reached menopause and 95 participants with incomplete information, 742 postmenopausal women were included in the final analysis. The specific inclusion and exclusion criteria for participants are detailed in Supplementary Figure S1 (available at https://weekly.chinacdc.cn/). For more comprehensive information about the study design, refer to the published study (*7*). Pollutant gases such as nitrogen dioxide (NO_2)

and ozone (O_3), along with $PM_{2.5}$ components like organic carbon (OC), elemental carbon (EC), water-soluble ions, and inorganic elements, were assessed using the closest fixed-site monitoring stations. Components that were detected below the limit of detection (<LOD) more than 25% of the time, including Br, Cs, Cu, Mo, Sc, Si, and Te, were excluded from our analysis. In cases where the components were undetectable (<LOD), we substituted half of the detection limit for the actual value. Serum samples were analyzed for sex hormone levels [T (testosterone) and E_2 (estradiol)] using automated biochemical analyzers after storage at −80 °C for a period of up to six months. Demographic information, physical characteristics, and lifestyle data were gathered through in-person interviews.

Spearman's correlations assessed the correlation matrix between $PM_{2.5}$ and its components. Generalized linear models elucidated the influences of $PM_{2.5}$ and its components on estradiol and testosterone levels. Time-lag patterns were identified by computing $PM_{2.5}$ concentrations at varying lag times (0-day, 1-day, 2-day, 3-day, 7-day, and 14-day). The most significant hormone level changes corresponding to each interquartile range (IQR) increase in $PM_{2.5}$ informed the selection of the lag period to investigate the impact of $PM_{2.5}$ components on sex hormones. Adjustments were made for multiple covariates, including: 1) demographic factors such as age, monitoring site, income, education, living status, and marital status; 2) lifestyle factors like smoking, alcohol consumption, vegetarianism, dietary supplements, and physical activity; 3) physical health indicators, including body mass index (BMI); 4) other airborne pollutants, namely O_3 and NO_2; and 5) meteorological conditions like relative humidity and ambient temperature. When examining $PM_{2.5}$ component effects on sex hormones, models were additionally controlled for $PM_{2.5}$ concentrations to mitigate confounding influences. Data analysis was performed using R version 3.6.1 (R Foundation for Statistical Computing, Vienna, Austria), with *P*-values adjusted for false discovery rate (FDR) in multiple comparisons. Statistical significance was determined at a two-sided *P*-value of less than 0.05.

Among the 742 postmenopausal women studied, the average age was 68.9±11.4 years. Their testosterone levels measured 0.68±1.81 nmol/L, while estradiol levels were 41.7±81.1 pmol/L. The majority had received 9 years or less of formal education, 77.9% were married, and 89.4% lived with others. Smoking prevalence was 4.4%, and alcohol consumption was reported by 2.2% of participants (Table 1). The average concentrations of $PM_{2.5}$, EC, and OC were 67.3 μg/m^3, 6.6 μg/m^3, and 12.0 μg/m^3. Further statistical details on $PM_{2.5}$ components, gaseous pollutants, and meteorological factors can be found in Supplementary Table S1 (available at https://weekly.chinacdc.cn/). In Supplementary Figure S2 (available at https://weekly.chinacdc.cn/), the Spearman's correlation matrix illustrates the relationships between 3-day average $PM_{2.5}$ exposures and its constituents, revealing mostly weak to moderate correlations, except for OC, Se, Pb, and Zn.

Figure 1 shows the lag pattern of associations between $PM_{2.5}$ and estradiol. The most significant effects were observed at a 3-day lag of exposure, followed by a gradual decrease over time, and eventually became statistically insignificant at longer lags. Each IQR increase in a 3-day lag period of $PM_{2.5}$ (38.6 μg/m^3) was associated with an elevated estradiol level of 24.7 pmol/L [95% confidence interval (*CI*): 9.47, 39.98 pmol/L] (Supplementary Table S2, available at https://weekly.chinacdc.cn/).

Our investigation revealed that a 3-day exposure to $PM_{2.5}$ and its components is worth a closer examination for their potential influence on sex hormone regulation. As demonstrated in Figure 2 and Supplementary Table S2, clear correlations were detected between sex hormone levels over the 3-day lag and specific $PM_{2.5}$ components, such as NH_4^+ [−55.22 (−92.21, −18.24) pmol/L], Cl^- [−21.63 (−40.13, −3.12) pmol/L], and Na^+ [26.27 (13.48, 39.05) pmol/L]. On the other hand, there were no notable relationships with other carbon fractions and water-soluble ions vis-à-vis estradiol levels. When examining inorganic elements, we found significant correlations with elevated sex hormone levels for Ag, As, Cd, Hg, Ni, Pb, Sb, Se, Sn, Tl, V, and Zn. However, after multiple comparison adjustments (FDRs>0.05), the positive links between Pb, and Zn exposures and estradiol were no longer statistically significant. Moreover, a rise in OC, As, Sb, and Sn exposure corresponded with an increase in testosterone levels, although these associations were attenuated following adjustment for FDR.

DISCUSSION

This research is the first to investigate how $PM_{2.5}$ and its particulate components affect reproductive hormone levels in postmenopausal women. A multi-

TABLE 1. Characteristics of the study population (*N*=742) in Beijing, Tianjin, and Hebei PLADs, China, 2018–2019.

Characteristics	*N* (or mean±SD)	% (or range)
Age (years)	68.9±11.4	43–91
<65	284	38.3
≥65	458	61.7
Education		
9 years or less	562	75.7
10 years or above	180	24.3
Marriage		
Married	578	77.9
Not married	164	22.1
Habitation		
Live alone	79	10.6
Live with others	663	89.4
Smoking		
No	709	95.6
Yes	33	4.4
Drinking		
No	726	97.8
Yes	16	2.2
Vegetarian diet		
No	678	91.4
Yes	64	8.6
Often use nutrient supplements		
No	660	88.9
Yes	82	11.1
Physical exercise		
No	240	32.3
Yes	502	67.7
BMI (kg/m^2)		
<28.0	567	76.4
≥28.0	175	23.6
Sex hormone biomarker		
Estradiol (pmol/L)	41.7±81.1	18.4–1,305
Testosterone (nmol/L)	0.68±1.81	0.087–32.1

Abbreviation: PLADs=provincial-level administrative divisions; *N*=number; SD=standard deviation.

center cross-sectional study revealed a delayed impact of $PM_{2.5}$ exposure on elevated sex hormones, particularly estradiol, with the most notable effect occurring 3 days after exposure. Various particulate components, especially water-soluble ions and inorganic elements such as Ag, As, Cd, Hg, Ni, Sb, Se, Sn, and Tl, were significantly associated with higher estradiol levels. These results have implications for future public health strategies to reduce the health risks related to $PM_{2.5}$ exposure in postmenopausal women.

Recent studies (*1*–*5*) have indicated an association between short-term $PM_{2.5}$ exposure and disruptions in reproductive hormone levels within China, particularly affecting estradiol, progesterone, and the T/E2 ratio (*1*). Consistent with prior research, our study found a significant positive correlation between $PM_{2.5}$ exposure with a 3-day lag and elevated estradiol levels. While some research has reported nonsignificant or negative associations between $PM_{2.5}$ exposure and sex hormone levels (*3*), these discrepancies may be attributable to varying $PM_{2.5}$ concentration levels, different chemical compositions, and unique characteristics of the study populations (*5*). It is important to note that the older adults in our study may exhibit increased sensitivity to $PM_{2.5}$-associated health effects due to their generally poorer health status, which could impair their ability to adapt to $PM_{2.5}$ exposure (*7*). Additionally, there was an observed increase in testosterone levels with higher exposure to As, Sb, and Sn, but the statistical significance of these relationships was lost after applying FDR adjustments. It appears that $PM_{2.5}$ may stimulate the secretion of estradiol and potentially modulate other sex hormones, such as testosterone, within the normal physiological range. This modulation is particularly relevant among postmenopausal women, considering their testosterone secretion is substantially lower than estradiol.

Several plausible mechanisms have been proposed to explain the adverse effects of $PM_{2.5}$ and its components on sex hormones. First, it is suggested that $PM_{2.5}$ exposure can stimulate the hypothalamic-pituitary-gonadal (HPG) axis, a key regulator of sex hormone secretion, thus potentially elucidating the observed associations (*5*). Second, exposure to $PM_{2.5}$ and its components may trigger the hypothalamic-pituitary-adrenal (HPA) axis, leading to reduced levels of testosterone and follicle-stimulating hormone (FSH) (*8*). Lastly, oxidative stress and inflammation pathways activated by $PM_{2.5}$ exposure, through a chemokine receptor-dependent mechanism, could contribute to the damage of sex hormones (*9*–*10*).

This study is subject to some limitations. First, the utilization of $PM_{2.5}$ measurements from monitoring sites as proxies for personal exposure likely led to exposure misclassification. Second, the assessment of sex hormone homeostasis was based on a single blood sample and only two indicators, which may not account for significant intra-individual variability given

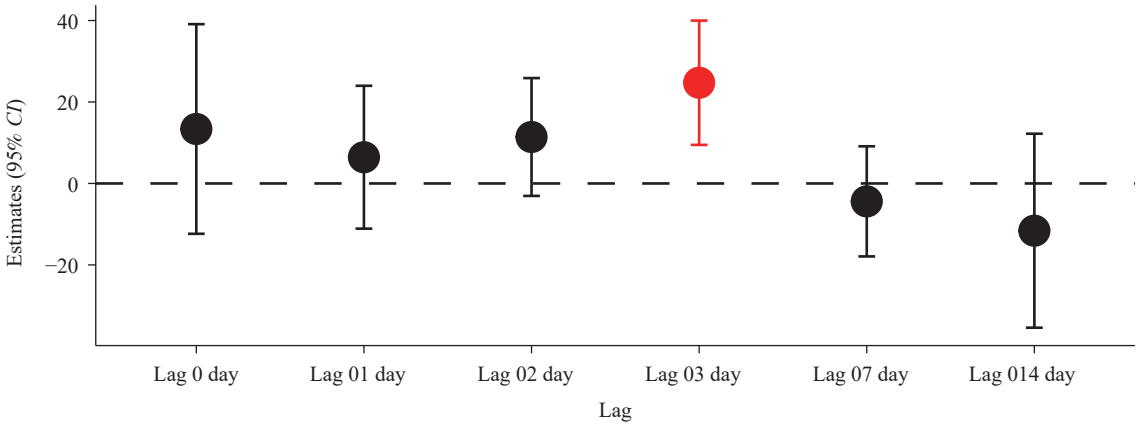

FIGURE 1. Changes (95% *CI*s) in estradiol associated with an IQR increase in $PM_{2.5}$ mass concentrations over various multiple-day lag periods in Beijing, Tianjin, and Hebei PLADs, China, 2018–2019.
Note: A significant association (*P*<0.05) was indicated by a red dot for confidence intervals (as bars), and black dots indicated statistically insignificant. Adjusted covariates include age, monitoring site, income level, education level, marital status, habitation status, smoking, drinking, vegetarian diet, nutrient supplements, physical exercise, BMI, temperature, relative humidity, ozone, and NO_2.
Abbreviation: *CI*=confidence interval; IQR=interquartile range; PLADs=provincial-level administrative divisions; NO_2=nitrogen dioxide; BMI=body mass index.

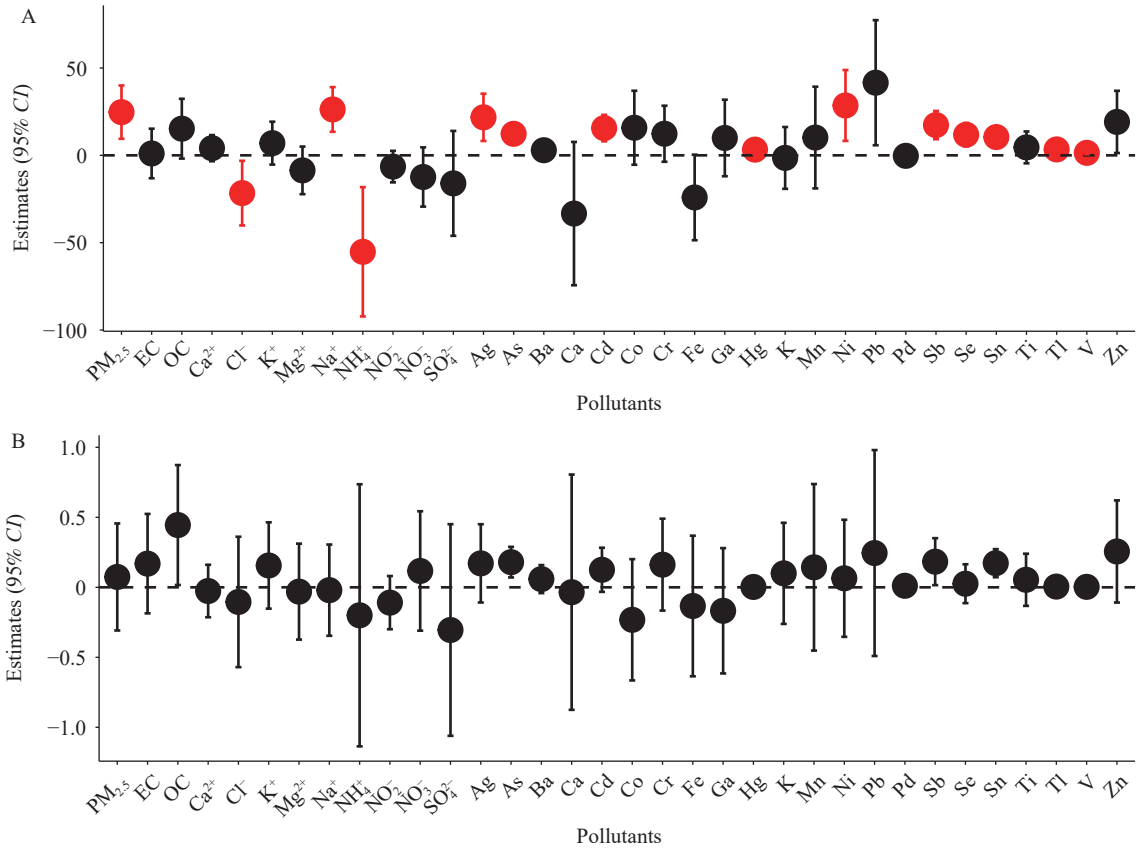

FIGURE 2. Changes (95% *CI*s) in sex hormones associated with an IQR increase in $PM_{2.5}$ and its constituents at a 3-day lag concentration prior to the investigation in Beijing, Tianjin, and Hebei PLADs,China, 2018–2019.
Note: Adjusted covariates in this study encompass various factors such as age, monitoring site, income level, education level, marital status, habitation status, smoking, drinking, vegetarian diet, nutrient supplements, physical exercise, BMI, temperature, relative humidity, ozone, and NO_2. Any statistically significant associations with adjusted *P*-values for FDR < 0.05 were indicated by red dots along with error bars; and black dots indicated statistically insignificant with adjusted *P*-values for FDR.
Abbreviation: E_2=estradiol; T=testosterone; *CI*=confidence interval; IQR=interquartile range; BMI=body mass index; NO_2=nitrogen dioxide; FDR=false discovery rate.

the sensitivity of serum sex hormones to environmental exposures. Third, the cross-sectional design precludes causal inferences and raises concerns about reverse causation due to the concurrent measurement of air pollution exposure and health outcomes. Fourth, potential unmeasured confounders, such as the participants' health status and external sources of estrogen-like soybean milk or bird's nest, may have influenced the results. Although the sample size was adequate to detect an association between $PM_{2.5}$ exposure and elevated sex hormone levels, it was not sufficiently large to uphold the association in the face of multiple comparisons. Fifth, the specificity of the results is somewhat limited, as other unaccounted variables may impact the findings and restrict the determination of a chronological relationship. Sixth, considering the epidemiological nature of the study, pinpointing a lag time between the impact on the organ system and the production and metabolism of hormones is challenging and may require further inquiry through animal studies underpinned by existing biological and epidemiological knowledge. Finally, the study focused on Chinese postmenopausal women with an average age of 68.9, meaning the findings may not extend to other ethnicities or younger age demographics.

In conclusion, this study presented the initial epidemiological evidence suggesting that even brief exposure to $PM_{2.5}$ could lead to a delayed increase in estradiol levels in postmenopausal women. Components of $PM_{2.5}$, particularly heavy metals like Ag, As, Cd, Hg, Ni, Sb, Se, Sn, Tl, and V, may be the primary contributors to elevated estradiol levels. However, no significant link between $PM_{2.5}$ and its components with testosterone levels was observed. These results underscore the importance of targeted interventions to minimize $PM_{2.5}$ exposure in postmenopausal women. Recommendations include reducing exposure to water-soluble ions and heavy metals, improving health literacy, conducting additional studies, implementing strategies to decrease $PM_{2.5}$ levels, and promoting personal protective measures.

Conflicts of interest: No conflicts of interest.

Funding: Supported by the National Natural Science Foundation of China (No. 82025030, No. 81941023), the National Key Research and Development Program of China (No. 2022YFC3702700), and the Open Fund provided by the Jiangsu Key Laboratory of Atmospheric Environment Monitoring and Pollution Control (KHK 2104).

doi: 10.46234/ccdcw2024.049

[#] Corresponding author: Xiaoming Shi, shixm@chinacdc.cn.

[1] Chinese Research Academy of Environmental Sciences, Beijing, China; [2] Collaborative Innovation Center of Atmospheric Environment and Equipment Technology, Jiangsu Key Laboratory of Atmospheric Environment Monitoring and Pollution Control (AEMPC), Nanjing University of Information Science & Technology, Nanjing City, Jiangsu Province, China; [3] China CDC Key Laboratory of Environment and Population Health, National Institute of Environmental Health, Chinese Center for Disease Control and Prevention, Beijing, China; [4] Department of Epidemiology and Health Statistics, School of Public Health, Capital Medical University, and Beijing Municipal Key Laboratory of Clinical Epidemiology, Beijing, China; [5] National Key Laboratory of Intelligent Tracking and Forecasting for Infectious Diseases, National Institute of Environmental Health, Chinese Center for Disease Control and Prevention, Beijing, China.

[&] Joint first authors.

Submitted: December 05, 2023; Accepted: March 07, 2024

REFERENCES

1. Wang FR, Chen Q, Zhan Y, Yang H, Zhang AH, Ling X, et al. Acute effects of short-term exposure to ambient air pollution on reproductive hormones in young males of the MARHCS study in China. Sci Total Environ 2021;774:145691. https://doi.org/10.1016/j.scitotenv.2021.145691.
2. Zhang YT, Li GL, Zhong YZ, Huang MQ, Wu JJ, Zheng JW, et al. 1, 2-Dichloroethane induces reproductive toxicity mediated by the CREM/CREB signaling pathway in male NIH Swiss mice. Toxicol Sci 2017;160(2):299 – 314. https://doi.org/10.1093/toxsci/kfx182.
3. Radwan M, Jurewicz J, Polańska K, Sobala W, Radwan P, Bochenek M, et al. Exposure to ambient air pollution-does it affect semen quality and the level of reproductive hormones? Ann Hum Biol 2016;43(1):50-6. http://dx.doi.org/10.3109/03014460.2015.1013986.
4. Checa Vizcaíno MA, González-Comadran M, Jacquemin B. Outdoor air pollution and human infertility: a systematic review. Fertil Steril 2016;106(4):897 – 904.e1. https://doi.org/10.1016/j.fertnstert.2016.07.1110.
5. Niu Y, Chen RJ, Xia YJ, Cai J, Ying ZK, Lin ZJ, et al. Fine particulate matter constituents and stress hormones in the hypothalamus-pituitary-adrenal axis. Environ Int 2018;119:186 – 92. https://doi.org/10.1016/j.envint.2018.06.027.
6. Chen C, Cai J, Wang CC, Shi JJ, Chen RJ, Yang CY, et al. Estimation of personal $PM_{2.5}$ and BC exposure by a modeling approach - results of a panel study in Shanghai, China. Environ Int 2018;118:194 – 202. https://doi.org/10.1016/j.envint.2018.05.050.
7. Tian YL, Fang JL, Wang F, Luo ZH, Zhao F, Zhang Y, et al. Linking the fasting blood glucose level to short-term-exposed particulate constituents and pollution sources: results from a multicenter cross-sectional study in China. Environ Sci Technol 2022;56(14):10172 – 82. https://doi.org/10.1021/acs.est.1c08860.
8. Snow SJ, Henriquez AR, Costa DL, Kodavanti UP. Neuroendocrine regulation of air pollution health effects: emerging insights. Toxicol Sci 2018;164(1):9 – 20. https://doi.org/10.1093/toxsci/kfy129.
9. Lavigne É, Burnett RT, Stieb DM, Evans GJ, Godri Pollitt KJ, Chen H, et al. Fine particulate air pollution and adverse birth outcomes: effect modification by regional nonvolatile oxidative potential. Environ Health Perspect 2018;126(7):077012. https://doi.org/10.1289/EHP2535.
10. Lafuente R, García-Blàquez N, Jacquemin B, Checa MA. Outdoor air pollution and sperm quality. Fertil Steril 2016;106(4):880 – 96. https://doi.org/10.1016/j.fertnstert.2016.08.022.

SUPPLEMENTARY MATERIAL

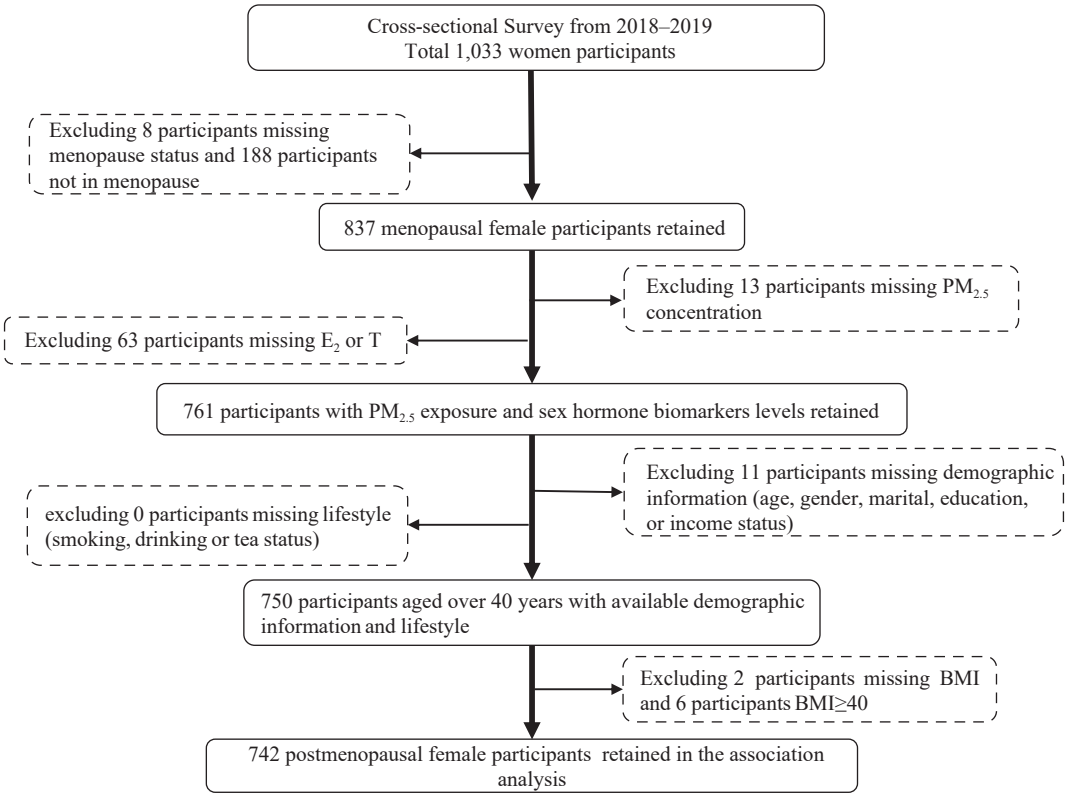

SUPPLEMENTARY FIGURE S1. Flow chart of study inclusion and exclusion criteria.
Abbreviation: E_2=estradiol; T=testosterone; BMI=body mass index.

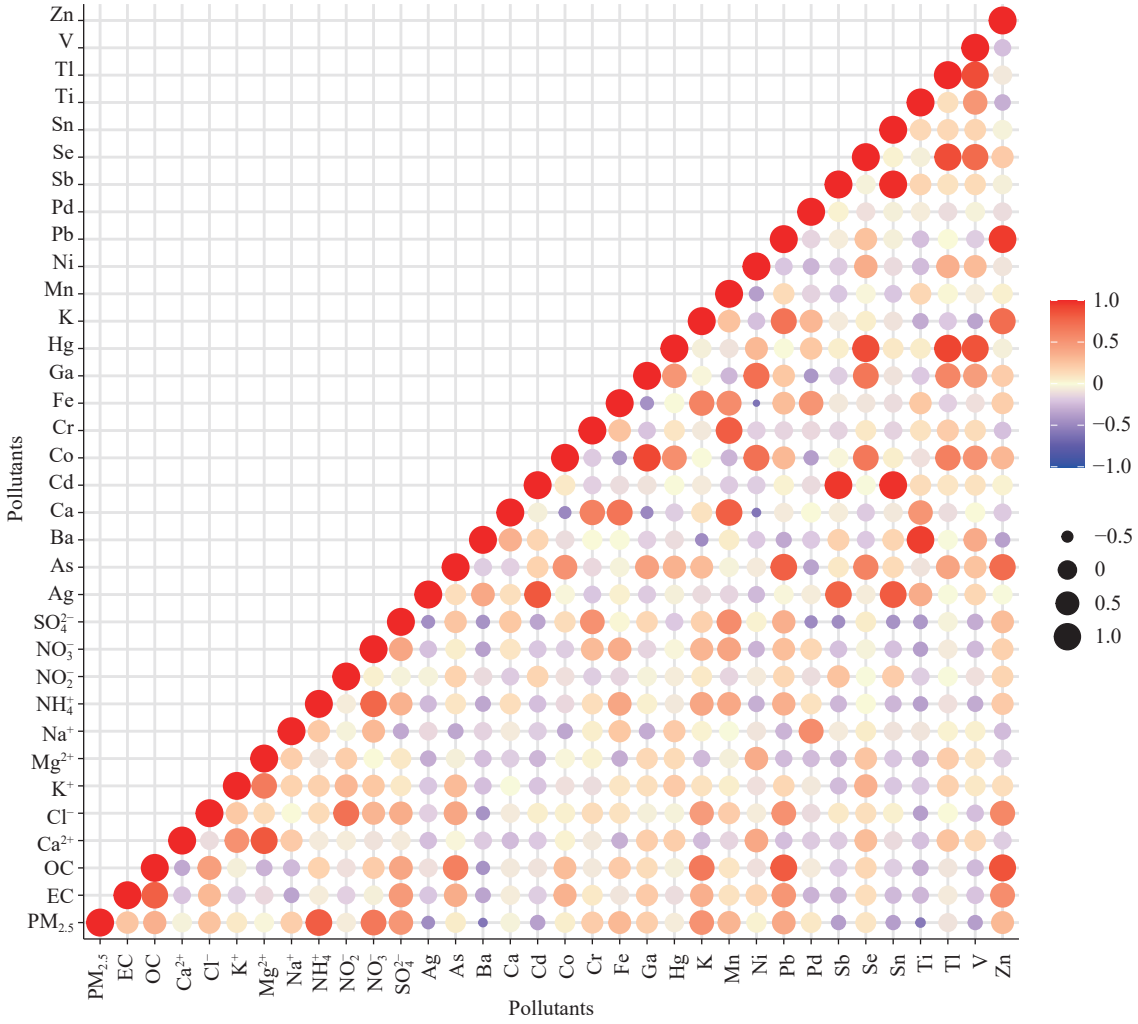

SUPPLEMENTARY FIGURE S2. Spearman's correlation matrix of 3-day average concentrations of $PM_{2.5}$ and its constituents.
Note: The magnitude of the Spearman's correlation coefficient was denoted by the size of dots, and black has no meaning. The color of dots from blue to red represents the change in the correlation from negative to positive.

SUPPLEMENTARY TABLE S1. Statistical description of the concentrations of $PM_{2.5}$, its chemical constituents, gaseous pollutants, and meteorological factors in Beijing, Tianjin, and Hebei PLADs, China, 2018–2019.

Exposures	Min	Max	Median	Mean	SD	IQR
$PM_{2.5}$ (μg/m^3)	14.9	121.3	66.9	67.3	27.3	38.6
Carbon fractions (μg/m^3)						
EC	0.86	29.40	2.97	6.60	6.84	8.17
OC	1.83	36.30	9.27	12.00	8.33	10.40
Water-soluble ions (μg/m^3)						
Ca^{2+}	0.12	16.10	0.58	1.86	3.39	1.87
Cl^-	0.33	8.91	2.35	2.41	1.82	2.49
K^+	0.06	5.60	0.68	0.96	1.04	1.17
Mg^{2+}	0.01	1.43	0.08	0.22	0.31	0.22
Na^+	0.15	5.65	0.71	0.98	0.91	0.49
NH_4^+	1.63	23.90	8.35	9.45	5.50	7.00
NO_2^-	0.04	7.78	0.17	1.03	1.54	1.57
NO_3^-	1.47	41.40	9.07	13.00	9.87	13.30
SO_4^{2-}	0.46	23.20	10.27	9.20	5.36	8.37
Inorganic elements (ng/m^3)						
Ag	0.50	85.50	4.53	10.70	16.90	13.70
As	0.33	159.00	9.37	17.00	26.00	12.70
Ba	5.36	287.00	23.10	43.70	67.70	17.70
Ca	16.60	999.00	451.70	479.00	251.00	379.00
Cd	0.04	104.00	4.18	11.70	21.00	9.61
Co	0.01	44.60	3.30	4.71	4.83	7.41
Cr	0.28	36.10	5.55	7.59	7.64	4.82
Fe	36.60	1,603.00	495.20	561.00	287.00	374.00
Ga	0.01	40.60	3.49	5.09	4.44	6.75
Hg	0.01	48.60	0.33	0.91	3.63	0.77
K	0.75	1,648.00	838.80	853.00	364.00	419.00
Mn	0.71	146.00	56.70	66.50	30.30	41.00
Ni	0.03	64.60	5.31	9.12	10.70	8.66
Pb	21.40	226.00	66.90	82.70	50.10	66.00
Pd	0.50	1,452.00	2.12	182.00	473.00	6.99
Sb	0.50	290.00	13.80	39.70	67.30	36.20
Se	1.29	84.60	7.37	7.66	6.21	3.87
Sn	0.50	330.00	15.80	35.50	64.90	24.30
Ti	2.86	205.00	35.80	49.50	47.90	23.20
Tl	0.01	109.00	2.01	2.57	7.94	1.61
V	0.06	113.00	0.68	2.60	9.01	0.66
Zn	76.80	744.00	238.70	282.00	169.00	139.00
Meteorological factors						
Temperature (°C)	−11.60	9.03	4.33	3.96	4.60	4.15
Relative humidity (%)	29.00	82.50	61.00	59.70	12.40	18.20
Gaseous pollutants (μg/m^3)						
NO_2	26.1	81.0	56.4	55.4	15.4	24.1
O_3	10.8	61.7	21.5	26.2	13.6	8.8

Abbreviation: PLADs=provincial-level administrative divisions; Min=minimum value; Max=maximum value; SD=standard deviation; IQR=interquartile range; EC=elemental carbon; OC=organic carbon; NO_2=nitrogen dioxide; O_3=ozone.

SUPPLEMENTARY TABLE S2. Betas and 95% *CI*s for E_2 based on each interquartile range (IQR) increase in the concentrations of $PM_{2.5}$ and its constituents.

Exposures	Beta (95% *CI*)	*P*	FDR
$PM_{2.5}$ (μg/m^3)	24.72 (9.47, 39.98)	<0.01	0.01
Carbon fractions (μg/m^3)			
EC	1.07 (−13.11, 15.25)	0.88	0.92
OC	15.26 (−1.85, 32.37)	0.08	0.15
Water−soluble ions (μg/m^3)			
Ca^{2+}	4.1 (−3.38, 11.57)	0.28	0.38
Cl^-	−21.63 (−40.13, −3.12)	0.02	0.05
K^+	6.97 (−5.3, 19.25)	0.27	0.36
Mg^{2+}	−8.61 (−22.23, 5.01)	0.22	0.31
Na^+	26.27 (13.48, 39.05)	<0.01	<0.01
NH_4^+	−55.22 (−92.21, −18.24)	<0.01	0.01
NO_2^-	−6.45 (−15.47, 2.57)	0.16	0.24
NO_3^-	−12.39 (−29.35, 4.56)	0.15	0.23
SO_4^{2-}	−16.06 (−46.07, 13.96)	0.29	0.39
Inorganic elements (ng/m^3)			
Ag	21.76 (8.21, 35.3)	<0.01	0.01
As	12.32 (7.04, 17.6)	<0.01	<0.01
Ba	2.93 (−1.97, 7.82)	0.24	0.34
Ca	−33.34 (−74.36, 7.67)	0.11	0.18
Cd	15.59 (8.01, 23.18)	<0.01	<0.01
Co	15.79 (−5.39, 36.97)	0.14	0.22
Cr	12.35 (−3.69, 28.39)	0.13	0.21
Fe	−24.11 (−48.59, 0.37)	0.05	0.10
Ga	9.93 (−11.97, 31.84)	0.37	0.46
Hg	3.27 (1.14, 5.4)	<0.01	0.01
K	−1.48 (−19.17, 16.21)	0.87	0.91
Mn	10.18 (−18.92, 39.29)	0.49	0.58
Ni	28.55 (8.26, 48.83)	0.01	0.02
Pb	41.58 (5.78, 77.38)	0.02	0.05
Pd	−0.29 (−2.22, 1.64)	0.77	0.85
Sb	17.32 (9.24, 25.41)	<0.01	<0.01
Se	11.8 (5.09, 18.5)	<0.01	<0.01
Sn	10.46 (5.6, 15.33)	<0.01	<0.01
Ti	4.55 (−4.55, 13.66)	0.33	0.42
Tl	3.38 (1.39, 5.37)	<0.01	<0.01
V	1.42 (0.61, 2.24)	<0.01	<0.01
Zn	19.13 (1.33, 36.93)	0.04	0.07

Abbreviation: E_2=estradiol; *CI*=confidence interval.

Preplanned Studies

Antimicrobial Resistance Analysis and Whole-Genome Sequencing of *Salmonella* Isolates from Environmental Sewage — Guangzhou City, Guangdong Province, China, 2022–2023

Bihui Su[1]; Guanghong Du[2]; Shuiping Hou[3]; Zongqiu Chen[3]; Xiaoying Wu[1]; Gang He[1]; Jun Yuan[3,#]; Chaojun Xie[4,#]

Summary

What is already known about this topic?

*S.*1,4,[5],12:i:- and *S.* Rissen are emerging serotypes of *Salmonella* that require close monitoring for antimicrobial resistance and containment of their spread.

What is added by this report?

The study aimed to identify antimicrobial resistance genes (ARGs) in *S.*1,4,[5],12:i:- and *S.* Rissen strains isolated from environmental sewage in Guangzhou City, Guangdong Province, China. A phylogenetic tree was constructed using single nucleotide polymorphism data to assess genetic relatedness among strains, offering insights for *Salmonella* infection outbreak investigations in the future.

What are the implications for public health practice?

It is crucial to implement strategies, such as integrating different networks, to control the spread of drug-resistant *Salmonella*. Novel technologies must be utilized to disinfect sewage and eliminate ARGs. Ensuring food safety and proper sewage disinfection are essential to curb the dissemination of *Salmonella*.

*S.*1,4,[5],12:i:- and *S.* Rissen are emerging *Salmonella* serotypes. Monitoring their antimicrobial resistance and controlling their spread is crucial. This study analyzed 35 *S.*1,4,[5],12:i:- and 6 *S.* Rissen isolates from untreated environmental sewage in Guangzhou. Resistance levels were tested, and whole-genome sequencing (WGS) was used to identify antimicrobial resistance genes (ARGs) and construct a phylogenetic tree to assess resistance and multi-drug resistance.

*S.*1,4,[5],12:i:- and *S.* Rissen were found to be more severe, carrying 183 ARGs related to various resistance mechanisms such as antibiotic efflux, target replacement, protection, inactivation, alteration, etc. It is noteworthy that the rare plasmid-mediated colistin resistance gene *mcr-3.1* was detected. This research contributes to the understanding of resistance in *S.*1,4,[5],12:i:- and *S.* Rissen, indicating that *Salmonella* is prevalent on both domestic and international scales. These findings are essential for establishing effective epidemiological data, informing clinical management practices, and devising appropriate public health strategies.

Sewage samples were obtained from various locations in 11 districts of Guangzhou City, Guangdong Province, China, such as hospitals, communities, markets, hotels, sewage plants, restaurants, and schools. 660 sewage samples were collected between February 1, 2022, and January 31, 2023, resulting in the isolation of 35 *S.*1,4,[5],12:i:- and 6 *S.* Rissen strains. The study included a total of 35 *S.*1,4,[5],12:i:- and 6 *S.* Rissen isolates. Antibiotic susceptibility testing was performed using a Gram-negative aerobic bacterial susceptibility testing plate from Shanghai Fosun Pharmaceutical Company, evaluating 17 antibiotics: β-lactams [Ampicillin (AMP), Ceftazidime (CAZ), Cefotaxime (CTX), Meropenem (MEM), Ertapenem (ETP)], β-lactamase inhibitors [Ampicillin-Sulbactam (AMS), Ceftazidime/avibactam (CZA)], Tetracyclines [Tetracycline (TET), Tigecycline (TIG)], Polymyxin [Colistin (CT)], Quinolones [Ciprofloxacin (CIP), Nalidixic acid (NAL)], Macrolides [Azithromycin (AZI)], Chloramphenicol [Chloramphenicol (CHL)], Aminoglycosides [Streptomycin (STR), Amikacin (AMK)], and Sulfonamides [trimethoprim/sulfamethoxazole (SXT)].

The micro broth dilution method was used to determine the susceptibility profiles of the isolates, classifying them as sensitive (S), intermediate (I), or resistant (R) in accordance with the standards set by the American Committee for Clinical Laboratory Standardization (CLSI). We defined multi-drug

resistance (MDR) as resistance to at least three different classes of antibiotics (*1*). The *Salmonella* isolates were submitted to Guangzhou Haotian Biotechnology Co., Ltd in China for WGS utilizing second-generation sequencing methods. Genome assembly of the sequencing data was performed using SPAdes (version 3.13.0; Algorithmic Biology Lab, St. Petersburg, Russia) software, allowing us to acquire the sequences of the *Salmonella* strains in FASTA format. To identify ARGs, we queried the assembled genomes against the CARD antibiotic resistance database (https://card.mcmaster.ca/). We constructed a whole-genome single nucleotide polymorphism (SNP) tree from the pan-SNPs generated by kSNP3.0, employing RAxML software with the General Time Reversible gamma substitution model and 1,000 bootstrap replicates for statistical support. This phylogenetic tree, annotated with antibiotic resistance genes, was visualized using the Interactive Tree of Life version 6 (iTOLv6; http://itol.embl.de/), including 12 reference *Salmonella* strains for comparison. The basic details of these reference strains are provided in Table 1.

For *S.*1,4,[5],12:i:- isolates, high rates of antimicrobial resistance were detected. Resistance was notably high against AMP (88.57%, 31/35), STR (88.57%, 31/35), TET (85.71%, 30/35), CHL (74.29%), SXT (71.43%, 26/35), and AMS (57.14%, 20/35). However, TIG (100%) and AMK (100%) showed complete sensitivity. MEM, ETP, CZA, CTX, CAZ, and AZI exhibited sensitivity rates exceeding 80%. All *S.* Rissen isolates displayed resistance to AMP (100%), TET (100%), CHL (100%), and SXT (100%), while being sensitive to MEM (100%), ETP (100%), CZA (100%), TIG (100%), AZI (100%), and AMK (100%). Among the 35 *S.*1,4,[5],12:i:- isolates, 32 were MDR, resulting in an MDR rate of 91.43%. Interestingly, 6 *S.*1,4,[5],12:i:- isolates exhibited resistance to five antimicrobials and had an MDR pattern of AMP-TET-CHL-STR-SXT. The MDR rate for *S.* Rissen was 100%. Complete details of the antimicrobial resistance profiles of *Salmonella* isolates are presented in Figure 1.

A total of 183 ARGs were identified in the genomes of *Salmonella* isolates (Table 2), encompassing various gene families such as resistance-nodulation-cell division (RND) antibiotic efflux pump, major facilitator superfamily (MFS) antibiotic efflux pump, and ATP-binding cassette (ABC) antibiotic efflux pump. These genes provide resistance to fluoroquinolones, cephalosporins, tetracyclines, and other antibiotics through mechanisms like efflux, target protection, and target alteration. The presence of known ARGs showed differing correlations with phenotypic resistance, with rates of 95.24%, 92.86%, and 83.33% for polymyxins, macrolides, and aminoglycosides, respectively. The correlation rates were lower for chloramphenicol antibiotics at 47.62%. The rates for β-lactams, tetracyclines, sulfonamides, β-lactam inhibitors, and quinolones were 76.19%, 66.67%, 64.29%, 59.52%, and 50.00%, respectively.

The phylogenetic tree of SNP analysis presented in Figure 2 displayed a clustering pattern where a local strain of *S.*1,4,[5],12:i:- and a strain of *S.* Muenster from U.S. cows grouped together, as did a local strain of *S.*1,4,[5],12:i:- and a strain of *S.* Enteritidis from U.S. chicken meat, indicating significant genetic

TABLE 1. Basic information on the 12 reference strains included in the phylogeny from Environmental Sewage — Guangzhou City, Guangdong Province, China, 2022–2023.

Number	Area	Time	Serotype	Source	NCBI number
Se40	Nanjing	2018	*S.* Enteritidis	Bird droppings	CP067369.1
ASM842900v2	America	2016	*S.* Muenster	Cow	CP082453.1
ASM1148075v2	America	2019	*S.* Typhimurium	Chicken breast	CP082526.1
ASM786162v2	America	2018	*S.* Enteritidis	Chicken breast	CP082565.1
C629	Qingdao	2014	*S.* Enteritidis	Chicken	CP015724.1
ATCC14028	Qingdao	2022	*S.* Typhimurium	Chicken	CP102669.1
WW012	Beijing	2016	*S.* Typhimurium	Pork	CP022168.1
SH160	Shanghai	2016	*S.* Typhimurium	Pork	CP053294.1
S29	Guangzhou	2014	*S.* Typhimurium	Hospital patient stool	CP085699.1
S34	Guangzhou	2014	*S.* Typhimurium	Hospital patient stool	CP086118.1
81741	Guangzhou	2015	*S.* Typhimurium	Hospital patient stool	CP019442.1
KNP01	Guangzhou	2000	*S.* Enteritidis	Hospital patient stool	CP113364.1

FIGURE 1. Resistance of *Salmonella* to 17 antibiotics (*n*=41) from Environmental Sewage—Guangzhou City, Guangdong Province, China, 2022–2023.
Abbreviation: CHL=chloramphenicol; SXT=trimethoprim/sulfamethoxazole; AMS=ampicillin-sulbactam; TET=tetracycline; AMP=ampicillin; STR=streptomycin; NAL=nalidixic acid; CT=colistin; CIP=ciprofloxacin; CTX=cefotaxime; CZA=ceftazidime; ETP=ertapenem; MEM=meropenem; TIG=tigecycline; AMK=amikacin; CAZ=ceftazidime; AZI=azithromycin.

similarity. Moreover, four *S.*1,4,[5],12:i:- isolates from Guangzhou wastewater were closely genetically linked to three *Salmonella* Typhimurium isolates from patient feces in Guangzhou hospitals during 2014 and 2015. Additionally, three strains of *S.*1,4,[5],12:i:- showed close genetic relationships with *Salmonella* Typhimurium, *Salmonella* Muenster, and *Salmonella* Enteritidis strains from the United States.

DISCUSSION

Salmonella represents a prevalent foodborne pathogen globally. The emergent trend of MDR, exacerbated by the misuse and overuse of antibiotics, has compromised treatment effectiveness and led to therapeutic failures (*2*). It is, therefore, vital to examine the resistance patterns and the genetic basis of antimicrobial resistance in *Salmonella*, with a focus on MDR, to better manage and contain infections. Notably, the serovars *S.*1,4,[5],12:i:- and *S.* Rissen have gained recognition as emerging threats to human health in various countries (*3–4*). There remains, however, a substantial gap in the understanding of these serovars' resistance profiles in China, particularly in Guangzhou. Our study aims to fill this crucial knowledge void. We conducted our research on *Salmonella* isolates obtained from environmental sewage, which offers distinctive insights. Conventional

TABLE 2. Predicted ARGs and resistance mechanisms in the genomes of *Salmonella* isolated (*n*=41) from Environmental Sewage — Guangzhou City, Guangdong Province, China, 2022–2023.

Resistance mechanism	ARG family	ARG
Antibiotic efflux	RND antibiotic efflux pump	*golS*, *mdsA*, *mdsB*, *YajC*, *sdiA*, *acrB Escherichia coli acrA*, *Shigella flexneri acrA*; *acrD*, *mdtA*, *mdtC*, *mdtB*, *CRP*, *mdtE*, *mdtF*, *gadX*, *rsmA*, *adeF*, *rsmA*, *OprN*, *OprJ*, *rsmA*, *OpmH*, *TriB*, *TriC*, *TriA*, *OpmD*, *OpmB*, *mdtB*, *cpxA*, *mdtM*, *baeR*, *baeS*, *OprM*, *Pseudomonas aeruginosa CpxR*; *MuxC*, *MuxB*, *MuxA*, *opmE*; *AcrF*, *AcrE*, *AcrS*
	MFS antibiotic efflux pump, RND antibiotic efflux pump	*H-NS*, *evgS*
	MATE transporter	*MdtK*, *PmpM*
	MFS antibiotic efflux pump	*mdtG*, *leuO*, *MexB*, *mdtN*, *mdtO*, *mdtP*, *Escherichia coli mdfA*, *emrY*, *mdtH*, *emrB*, *emrR*, *emrA*, *emrK*, *Escherichia coli mdfA*, *floR*, *cmlA1*, *cmlA5*, *cmlA6*, *tetR*, *tet (A)*, *tet (B)*, *tet (M)*, *bcr-1*, *qacEdelta1*
	ABC antibiotic efflux pump	*msbA*; *YojI*
	SMR antibiotic efflux pump	*Klebsiella pneumoniae KpnF*, *Klebsiella pneumoniae KpnE*, *Klebsiella pneumoniae Kpn*, *Klebsiella pneumoniae KpnH*; *qacL*
	kdpDE	*kdpE, Type A NfxB*
Antibiotic target replacement and antibiotic target protection	Sulfonamide resistant sul; trimethoprim resistant dihydrofolate reductase dfr qnr; msr-type ABC-F protein	*sul1*, *sul2*, *sul3*; *dfrA1*, *dfrA12*, *dfrA14*, *dfrA27*, *QnrB6*, *QnrD1*, *QnrS1*; *msrE*
Antibiotic inactivation	ANT (3"); AAC (3); TEM beta-lactamase; AAC (6'); PDC beta-lactamase; fosfomycin thiol transferase; OXA beta-lactamase; CTX-M beta-lactamase; APH (6); APH (4); APH (3'); APH (3"); CAT; EC beta-lactamase; CARB beta-lactamase; CMH beta-lactamase; MPH; LNU; rifampin ADP-ribosyltransferase (Arr); DHA beta-lactamase;	*aadA2*, *aadA*, *aadA22*, *aadA16*, *aadA3*, *ANT (3")-IIa*; *AAC (3)-IId*, *AAC (3)-IVa*; *TEM-1*, *TEM-169*; *AAC (6')-Iy*, *AAC(6')-Iaa* , *AAC (6')-Ib-cr6*; *PDC-11*, *PDC-3*; *FosA*, *FosA8*, *FosA2*, *FosA7*; *OXA-846*, *OXA-904*, *OXA-1*, *OXA-10*;*CTX-M-55*, *CTX-M-65*; *CTX-M-3*; *APH (6)-Id*; *APH (4)-Ia*; *APH (3')-IIb*, *APH (3')-Ia*; *APH (3")-Ib*; *Pseudomonas aeruginosa catB7catB3*; *EC-13*; *Escherichia coli ampC beta-lactamase*, *CARB-3*; *catA4*; *CMH-3*; *mphA*, *Mrx*; *linG*, *lnuF*; *arr-2*, *arr-3*; *DHA-1*
Antibiotic target alteration	Undecaprenyl pyrophosphate related proteins; glycopeptide resistance gene cluster, Van ligase; pmr phosphoethanolamine transferase; antibiotic-resistant UhpT; Penicillin-binding protein mutations conferring resistance to beta-lactam antibiotics; antibiotic-resistant GlpT; elfamycin resistant EF-Tu; vanW, glycopeptide resistance gene cluster; pmr phosphoethanolamine transferase;pmr phosphoethanolamine transferase; MCR phosphoethanolamine transferase	*bacA*; *vanG*; *PmrF*, *ArnT*, *arnA*, *cprR*, *cprS*, *basR*; *Escherichia coli UhpT with mutation conferring resistance to fosfomycin*; *Haemophilus influenzae PBP3 conferring resistance to beta-lactam antibiotics*; *Escherichia coli GlpT with mutation conferring resistance to fosfomycin*; *Escherichia coli EF-Tu mutants conferring resistance to Pulvomycin*; *vanW gene in vanG cluster*; *eptA*; *ugd*; *MCR-3.1*
Antibiotic efflux, reduced permeability to antibiotic	RND antibiotic efflux pump, General Bacterial Porin with reduced permeability to beta-lactams; RND antibiotic efflux pump, Opr	*marA*, *ramA*; *ParS*, *ParR*
Antibiotic target alteration, antibiotic efflux	RND antibiotic efflux pump; pmr phosphoethanolamine transferase	*Escherichia coli AcrAB-TolC with MarR mutations conferring resistance to ciprofloxacin and tetracycline*; *cprS*, *basS*

Abbreviation: ARG=antimicrobial resistance gene; RND=resistance-nodulation-cell division; MFS=major facilitator superfamily; MATE=multidrug and toxic compound extrusion; ABC=ATP-binding cassette; SMR=small multidrug resistance; qnr=quinolone resistance protein; CAT=chloramphenicol acetyltransferase; CARB beta-lactamase=ampC-type beta-lactamase; MPH=macrolide phosphotransferase; LNU=lincosamide nucleotidyltransferase; Arr=rifampin ADP-ribosyltransferase; CMH=neutral glycosphingolipids; OXA=oxidase assembly; ADP=adenosine diphosphate; DHA=dhahran; MCR=mobile colistin resistance; Opr=outer membrane porin; PDC=pseudomonas-derived cephalosporinase; EF-Tu=elongation factor thermo-unstable; msr=methionine sulfoxide reductase; ANT=aminoglycoside nucleotidyl transferase; qnr=quinolone resistance; MCR=mobile colistin resistance.

antimicrobial resistance surveillance primarily targets symptomatic clinical cases, thereby overlooking asymptomatic carriers and key environmental reservoirs including livestock, vegetables, and water bodies. Conversely, environmental sewage likely harbors *Salmonella* strains shed from multiple sources, offering a more comprehensive overview of the strains present. Additionally, we utilized SNP analysis to elucidate the genetic relationships among isolates, providing valuable data for tracing the origins of potential *Salmonella* outbreaks in the future.

In this study, we found that both *S.*1,4,[5],12:i:- and

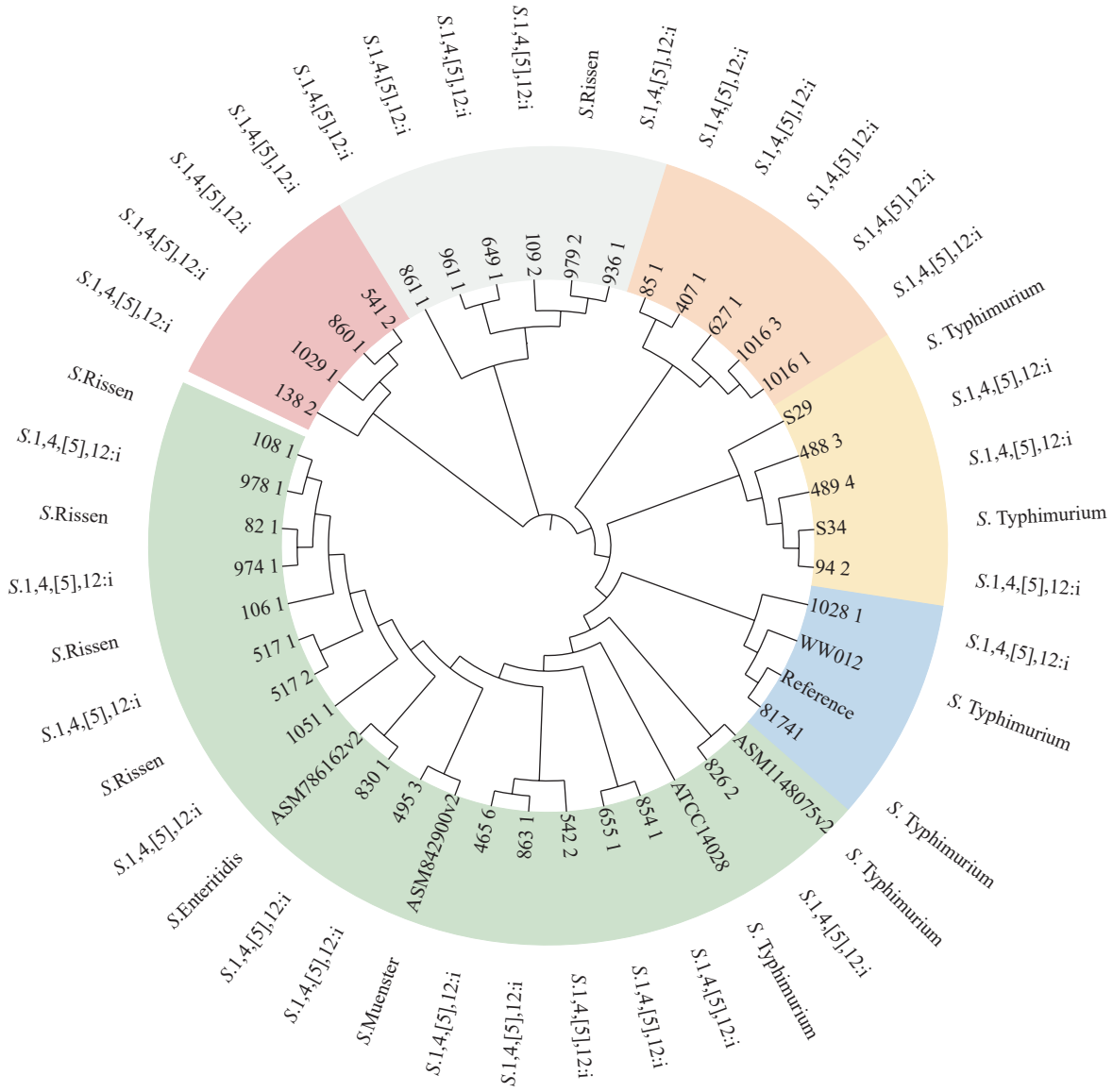

FIGURE 2. A phylogenetic tree illustrating the evolutionary relationship of *Salmonella* strains isolated from Guangzhou's environmental wastewater using whole-genome SNPs.
Abbreviation: SNP=single nucleotide polymorphism.

S. Rissen isolates exhibited high resistance levels to commonly prescribed clinical antibiotics, such as AMP, STR, CHL, SXT, AMS, as well as to TET, an antibiotic critically important in veterinary medicine. These findings underscore the need for judicious use of these antibiotics in both human medicine and animal farming to prevent treatment failures. However, antibiotics such as TIG, AMK and CZA have demonstrated high antimicrobial sensitivity and thus may offer effective treatment options. The extremely high prevalence of multidrug resistance observed in these isolates is alarming, with potential severe implications for both human health and life. A comprehensive strategy that integrates bacterial and fungal resistance surveillance, clinical prescription monitoring, and hospital infection control is essential to combat the spread of drug-resistant pathogens (*5*).

Drug efflux pumps are integral membrane proteins that actively expel antibiotics from the cell, representing a significant mechanism contributing to the MDR observed in Gram-negative bacteria (*1*). Our investigation identified six types of efflux pumps in both *S.*1,4,[5],12:i:- and *S.* Rissen isolates: the RND family, ABC superfamily, MFS, SMR family, MATE, and kdpDE. These systems are likely involved in the extensive antibiotic resistance demonstrated by *S.*1,4,[5],12:i:- and *S.* Rissen isolates. In addition, we discovered the *mcr-3.1* subtype of the plasmid-

mediated colistin resistance gene *mcr-3*, which has been infrequently reported in China (*6*). Literature suggests that *mcr-3.1* is instrumental in propagating drug resistance via both plasmid transfer, or horizontal transmission, and chromosomal insertion, or vertical transmission (*7*). Ongoing surveillance of *mcr-3.1* is vital to controlling its dissemination within China. Furthermore, our WGS analysis predicted genes responsible for resistance to fluoroquinolones, aminoglycosides, and tetracyclines, among others. Notably, there was a discernible correlation between the presence of these ARGs and the corresponding resistance phenotypes, underscoring the importance of ARGs in *Salmonella* resistance and the reduction in antibiotic efficacy.

Antibiotic-resistant bacteria (ARB), ARGs, and mobile genetic elements (MGEs), such as plasmids, are present in sewage and promote the horizontal transfer of ARGs among various microorganisms, leading to increased bacterial resistance (*8*). This study has identified numerous ARGs; consequently, their eradication from sewage is of paramount importance. Traditional disinfection methods, including chlorine, ozone, and ultraviolet light, exhibit minimal effectiveness in eliminating ARGs. While the combined photocatalytic oxidation-membrane bioreactor (MBR) process has proven effective at removing ARGs in laboratory studies, its application in real-world settings remains impractical (*9*). Therefore, there is an urgent need to develop innovative disinfection technologies suited for the efficient removal of ARGs from sewage.

The phylogenetic analysis indicates that *Salmonella* possesses the capability to disseminate various sources and geographical areas, including across international borders. The primary transmission vectors for *Salmonella* include contaminated food, water, and the international trade of animal feed (*10*). To mitigate the dissemination of *Salmonella*, it is imperative to enforce stringent food safety inspection protocols that encompass both food products and animal feed. Concurrently, the disinfection of environmental wastewater is of paramount importance.

This study is subject to some limitations due to the small sample size, which comprised only 35 *S.*1,4,[5],12:i:- isolates and 6 *S.* Rissen isolates. Consequently, these numbers may not sufficiently reflect the overall resistance features of these two *Salmonella* serotypes. In addition, owing to the limitations of second-generation genome sequencing methods for WGS, it's impossible to obtain the location of resistance genes, such as whether it's on the chromosomes or plasmids, which will limit further study on the resistance mechanism of Salmonella.

Nonetheless, the breadth of the sewage sample sources — from seven locations across eleven districts in Guangzhou city — lends some degree of representativeness to the findings. Additionally, the collection of sewage samples was carried out by trained professionals and the samples were transported to the laboratory for analysis within 48 hours, stored at 4 °C. The methodological procedures, including selective enrichment, isolation, morphological examination, biochemical testing, and serological typing, were methodically performed to ensure the isolation of *Salmonella* strains. The thoroughness of the experimental protocol supports the accuracy of the results.

Conflicts of interest: No conflicts of interest.

Funding: Supported by Guangdong Basic and Applied Basic Research Foundation (2021A1515012539), Science and Technology Program of Guangzhou, China (202102080295), Guangzhou Key Medical Discipline (2021-2023-11), 2023 Huadu District Medical and Health General Scientific Research Special Project of Guangzhou Huadu District Bureau of Science, Technology, Industry, Commerce, and Information Technology (23-HDWS-079), Key R&D Plan of Guangzhou Science and Technology Project (202206080003), and Guangzhou Science and Technology Plan Project (2023A03J0938).

doi: 10.46234/ccdcw2024.050

[#] Corresponding authors: Jun Yuan, yuanjuncom@163.com; Chaojun Xie, 35451900@qq.com.

[1] Tuberculosis Management and Treatment Department, Guangzhou Chest Hospital, Guangzhou City, Guangdong Province, China; [2] School of Public Health, Guangzhou Medical University, Guangzhou City, Guangdong Province, China; [3] Guangzhou Center for Disease Control and Prevention, Guangzhou City, Guangdong Province, China; [4] Office of the Director, Huadu District Center for Disease Control and Prevention, Guangzhou City, Guangdong Province, China.

Submitted: December 28, 2023; Accepted: February 29, 2024

REFERENCES

1. Nang SC, Li J, Velkov T. The rise and spread of *mcr* plasmid-mediated polymyxin resistance. Crit Rev Microbiol 2019;45(2):131 – 61. https://doi.org/10.1080/1040841X.2018.1492902.
2. Borah P, Dutta R, Das L, Hazarika G, Choudhury M, Deka NK, et al. Prevalence, antimicrobial resistance and virulence genes of *Salmonella* serovars isolated from humans and animals. Vet Res Commun 2022;46(3):799 – 810. https://doi.org/10.1007/s11259-022-09900-z.

3. Qin XJ, Yang MZ, Cai H, Liu YT, Gorris L, Aslam MZ, et al. Antibiotic resistance of *Salmonella* typhimurium monophasic variant 1, 4,[5],12:i:-in China: a systematic review and meta-analysis. Antibiotics (Basel) 2022;11(4):532. https://doi.org/10.3390/antibiotics11040532.
4. Elbediwi M, Shi DW, Biswas S, Xu XB, Yue M. Changing patterns of *Salmonella* enterica serovar rissen from humans, food animals, and animal-derived foods in China, 1995-2019. Front Microbiol 2021;12:702909. https://doi.org/10.3389/fmicb.2021.702909.
5. Guo Y, Ding L, Yang Y, Han RR, Yin DD, Wu S, et al. Multicenter antimicrobial resistance surveillance of clinical isolates from major hospitals - China, 2022. China CDC Wkly 2023;5(52):1155 – 60. https://doi.org/10.46234/ccdcw2023.217.
6. Yu K, Wang HY, Cao ZZ, Gai YD, Liu M, Li GQ, et al. Antimicrobial resistance analysis and whole-genome sequencing of *Salmonella* enterica serovar Indiana isolate from ducks. J Glob Antimicrob Resist 2022;28:78 – 83. https://doi.org/10.1016/j.jgar.2021.12.013.
7. Lee S, An JU, Kim WH, Yi S, Lee J, Cho S. Different threats posed by two major mobilized colistin resistance genes— *mcr-1.1 and mcr-3.1* — revealed through comparative genomic analysis. J Glob Antimicrob Resist 2023;32:50 – 7. https://doi.org/10.1016/j.jgar.2022.12.007.
8. Wang JQ, Xu SQ, Zhao K, Song G, Zhao SN, Liu RP. Risk control of antibiotics, antibiotic resistance genes (ARGs) and antibiotic resistant bacteria (ARB) during sewage sludge treatment and disposal: a review. Sci Total Environ 2023;877:162772. https://doi.org/10.1016/j.scitotenv.2023.162772.
9. Pazda M, Kumirska J, Stepnowski P, Mulkiewicz E. Antibiotic resistance genes identified in wastewater treatment plant systems - a review. Sci Total Environ 2019;697:134023. https://doi.org/10.1016/j.scitotenv.2019.134023.
10. Li Y, Teng L, Xu XB, Li XM, Peng XQ, Zhou X, et al. A nontyphoidal *Salmonella* serovar domestication accompanying enhanced niche adaptation. EMBO Mol Med 2022;14(11):e16366. https://doi.org/10.15252/emmm.202216366.

Preplanned Studies

Molybdenum Concentration and the Risk of Spontaneous Preterm Birth: A Nested Case-Control Study — Beijing Municipality, China, 2018–2020

Junhua Huang[1]; Wei Zheng[1]; Aili Wang[1,2]; Weiling Han[1]; Junxi Chen[3,4]; Hang An[3,4]; Lailai Yan[5]; Zhiwen Li[3,4,#]; Guanghui Li[1,#]

Summary

What is already known about this topic?

The level of molybdenum (Mo) in a mother's urine has been linked to the growth rate of the fetus and the blood pressure levels in children.

What is added by this report?

We evaluated the variations in maternal plasma Mo concentrations throughout pregnancy and their potential association with the risk of spontaneous preterm birth (SPB).

What are the implications for public health practice?

Future research must determine the Mo levels in pregnant women across various regions in China. Moreover, particular attention needs to be given to the potential increase in Mo concentration throughout pregnancy and its possible adverse impacts on the health of both the mother and the fetus.

Spontaneous preterm births (SPB), with no identifiable causes, account for a significant 60%–70% of all preterm births (*1*). These are responsible for about 35% of neonatal fatalities linked to premature births (*2*). Given its high incidence and consequences, the prevention of preterm births is increasingly gaining traction as a critical public health concern. An essential ultratrace element, molybdenum (Mo), plays a role in several human metalloflavoproteins. Studies have revealed that the maternal urinary Mo concentration during pregnancy bears an inverse association with fetal abdominal circumference and estimated fetal weight while also positively correlating with childhood blood pressure (*3*–*4*). This study aimed to monitor Mo levels in pregnant women's plasma and analyze any potential link to SPB risk. We found the maternal plasma Mo concentration in the SPB group was significantly greater than that in the control group during the first trimester [2.12 (1.56–2.69) *vs.* 2.02 (1.46–2.50) ng/mL, *P*=0.027]. Higher Mo levels (≥ 2.584 ng/mL) recorded in the first trimester were linked with an elevated SPB risk after adjusting for maternal age, ethnicity, pre-pregnancy body mass index (PPBMI), parity, mode of delivery, education, and income levels [odds ratio (*OR*)=2.074 (1.212, 3.550), *P*=0.008]. However, when the Mo concentration stood at ≥3.554 ng/mL during the third trimester, the *OR* for SPB reached 1.732 (1.016, 2.953), *P*=0.044, again adjusted for the aforementioned factors. Furthermore, it is crucial to note that the current reference range for blood Mo concentrations in pregnant women across various Chinese regions remains undefined. Hence, clinicians must be vigilant against illnesses potentially arising from high Mo concentrations.

We conducted a nested case-control study with subjects drawn from the Beijing birth cohort. In estimating our sample size, we predicated on a high-level Mo exposure rate of approximately 50% in the term delivery group, a common odds ratio of 2 (*5*), a two-sided importance level of α =0.05 and β=0.10, and a case-control proportion of 1∶1. Calculations performed using the PASS (version 11.0; NCSS statistical software, Kaysville, USA), indicated a minimum sample size of 179 patients required for the SPB group. Eligibility criteria included women aged between 18 and 44 years willing to undergo routine prenatal examinations and deliveries at the Beijing Obstetrics and Gynecology Hospital, and who provided signed consent. Following an overnight fast (≥8 hours), we obtained 2.0 mL venous blood samples from each participant during the first (7 to 9 weeks of gestation) and third trimesters (33 to 34 weeks). SPB was defined as preterm birth with intact fetal membranes and preterm premature rupture of membranes before the 37th week of gestation, excluding iatrogenic preterm birth caused by medical interventions such as maternal fetal induction or

cesarean section. After excluding women with twin pregnancies, cervical inadequacies, a history of preterm birth, placental abruption, iatrogenic preterm birth due to hypertension, diabetes, central placental previa, abnormal liver function, acute fatty liver, cholestasis, appendicitis, and significant cardiac insufficiency, liver, kidney, and brain diseases, as well as those on bed-rest; we selected a cohort of 29,303 live singletons, 617 of whom were SPB cases. We further narrowed it down to 236 SPB patients who had blood samples collected during both the first and third trimesters. A control group of 236 subjects composed of healthy pregnant women with gestational weeks of <39 or >41 was also selected (Supplementary Figure S1, available athttps://weekly.chinacdc.cn/). The study was granted approval by the Ethics Committee of the Beijing Obstetrics and Gynecology Hospital, Capital Medical University.

The Mo concentrations were determined using inductively coupled plasma mass spectrometry (ICP-MS, ELAN DRC II, PerkinElmer, USA). Standardized plasma (ClinChek® - Plasma Control, Level II, Germany) samples served as controls for quality assurance. The detection limit (LOD) for Mo in the plasma was set at 0.04 ng/mL and our analysis found that the concentrations of Mo in all samples exceeded this threshold. In the standard plasma samples, the median reference value for Mo was 5.96 ng/mL, ranging from a minimum of 4.77 ng/mL to a maximum of 7.15 ng/mL. To investigate the correlation between Mo levels and the risk of SPB anomalies, we executed an unconditional logistic regression analysis utilizing the IBM SPSS Statistics software (version 26.0; IBM Corporation, Armonk, NY, USA). We deemed a two-tail *P*-value of less than 0.05 as statistically significant in all statistical analyses.

The study groups, consisting of 236 patients each in the SPB cohort and the control group, demonstrated comparable demographic characteristics with respect to maternal education, personal monthly income, maternal ethnicity, and fetal gender. Nevertheless, significant differences were observed concerning maternal delivery time (35.53±0.69 weeks for SPB *vs.* 39.70±0.74 weeks for controls, *P*<0.001), maternal age [under 35 years: 177 (75%) SPB *vs.* 196 (83.05%) controls; 35 years and older: 59 (25%) SPB *vs.* 40 (16.95%) controls, *P*=0.032], PPBMI [under 18.5 kg/m^2: 29 (12.29%) SPB *vs.* 29 (12.29%) controls; 18.5–25 kg/m^2: 149 (63.14%) SPB *vs.* 176 (74.58%) controls; 25 kg/m^2 and above: 58 (24.57%) SPB *vs.* 31 (13.13%) controls, *P*=0.021], parity [nulliparous: 154 (65.25%) SPB *vs.* 184 (77.97%) controls; multiparous: 82 (34.75%) SPB *vs.* 52 (22.03%) controls, *P*=0.002], mode of delivery [vaginal: 145 (61.44%) SPB *vs.* 176 (74.58%) controls; cesarean section: 91 (38.56%) SPB *vs.* 60 (25.42%) controls, *P*=0.002], fetal birth weight (2696.46±338.75 g SPB *vs.* 3429.94±299.46 g controls, *P*<0.001), and birth length (47.70±1.93 cm SPB *vs.* 50.25±0.90 cm controls, *P*<0.001) (Table 1).

During the first trimester, median maternal plasma Mo concentrations were measured at 2.07 (1.53–2.58) ng/mL for the entire cohort. Within this cohort, women in the SPB group had a slightly higher median Mo concentration of 2.12 (1.56–2.69) ng/mL compared to 2.02 (1.46–2.50) ng/mL in the control group, and this difference was statistically significant (*P*=0.027). By the third trimester, the overall median Mo concentration had increased to 2.59 (1.66–3.55) ng/mL. The SPB group's median concentration rose to 2.66 (1.69–3.69) ng/mL, while the control group's median was 2.54 (1.58–3.41) ng/mL, though this inter-group difference was not statistically significant (*P*=0.147). Notably, third trimester Mo concentrations were significantly elevated when compared to first trimester levels (*P*<0.001). Between the first and third trimesters, the SPB group experienced an increase in Mo concentration of 0.37 (range: −0.86 to 1.73) ng/mL and the control group an increase of 0.35 (range: −0.84 to 1.73) ng/mL, with no significant difference between the groups (*P*=0.775) (Table 2).

During the first trimester, when maternal plasma Mo concentration was at or above 2.584 ng/mL, the odds of SPB as determined by logistic regression analyses with various adjustments, were significantly increased with *OR*s of 1.878 [95% confidence interval (*CI*): 1.129, 3.124, *P*=0.015], 1.892 (95% *CI*: 1.118, 3.201, *P*=0.018), and 2.074 (95% *CI*: 1.212, 3.550, *P*=0.008). In the third trimester, the occurrence of SPB at a Mo concentration of 3.554 ng/mL or higher had an adjusted *OR* of 1.732 (95% *CI*: 1.016, 2.953, *P*=0.044), after factoring in variables such as maternal age, ethnicity, PPBMI, number of births (parity), mode of delivery, educational background, and income levels. In comparison to the lowest quartile of plasma Mo levels, the odds of experiencing SPB were 1.217 (95% *CI*: 0.715, 2.072), 1.084 (95% *CI*: 0.635, 1.848), and 2.074 (95% *CI*: 1.212, 3.550) for the second, third, and fourth quartiles, respectively, showing a significant trend (P_{trend}=0.017) in the third logistic regression model. In the first trimester, the P_{trend} values for the remaining two models were 0.036

TABLE 1. Characteristics of women in the SPB and control groups.

Characteristics	SPB (*n*=236)	Control (*n*=236)	*P*
Delivery time (weeks) (mean±SD)	35.53±0.69	39.70±0.74	<0.001*
Age (year), *n* (%)			0.032*
<35	177 (75)	196 (83.05)	
≥35	59 (25)	40 (16.95)	
PPBMI (kg/m^2), *n* (%)			0.021*
<18.5	29 (12.29)	29 (12.29)	
18.5–25	149 (63.14)	176 (74.58)	
≥25	58 (24.57)	31 (13.13)	
Parity, *n* (%)			0.002*
0	154 (65.25)	184 (77.97)	
≥1	82 (34.75)	52 (22.03)	
Education, *n* (%)			0.130
<Bachelor's degree	63 (26.69)	49 (20.76)	
≥Bachelor's degree	173 (73.31)	187 (79.24)	
Personal monthly income (CNY), *n* (%)			0.271
<10,000	58 (24.58)	48 (20.34)	
≥10,000	178 (75.42)	188 (79.66)	
Ethnicity, *n* (%)			0.616
Han	215 (91.10)	218 (92.37)	
Other ethnicities	21 (8.90)	18 (7.63)	
Delivery way, *n* (%)			0.002*
Vaginal delivery	145 (61.44)	176 (74.58)	
Cesarean section	91 (38.56)	60 (25.42)	
Birth weight (g) (mean±SD)	2696.46±338.75	3429.94±299.46	<0.001*
Birth length (cm) (mean±SD)	47.70±1.93	50.25±0.90	<0.001*
Fetal gender, *n* (%)			0.310
Boy	132 (55.93)	121 (51.27)	
Girl	104 (44.07)	115 (48.73)	

Abrreviation: SPB=spontaneous preterm birth; Mo=molybdenum; PPBMI=pre-pregnancy body mass index; CNY=Chinese Yuan.
* P<0.05.

and 0.039, respectively. For the third trimester, P_{trend} was found to be significant at 0.038 in logistic regression model 3 (Table 3).

The subgroup analysis results suggested a correlation between plasma Mo concentration and the risk of SPB in overweight, obese, and multiparous mothers during the first trimester (Supplementary Tables S1 and S2, available at https://weekly.chinacdc.cn/). Additionally, our sensitivity analysis results corroborate with our preliminary findings (Supplementary Table S3, available at https://weekly.chinacdc.cn/).

DISCUSSION

Our results indicate a positive correlation between elevated levels of Mo in maternal plasma and an amplified risk of SPB during the first trimester, specifically in multiparous or overweight/obese women. Although these findings are suggestive, additional studies are necessary to clarify the exact mechanisms by which Mo affects SPB. Considering these results, it is essential to enhance awareness around Mo consumption and environmental exposure during early pregnancy due to their potential contribution to SPB risk.

Our study showed an elevated risk of SPB with observed Mo concentrations of ≥2.584 ng/mL in the first trimester and ≥3.554 ng/mL in the third trimester. Comparisons with other studies provides additional context. For example, the National Institute of Child Health and Human Development (NICHD)

TABLE 2. Median concentrations of molybdenum in maternal plasma.

Groups	Total M (IQR)	SPB M (IQR)	Control M (IQR)	$P^{\dagger}$
Plasma				
1st	2.07 (1.53–2.58)	2.12 (1.56–2.69)	2.02 (1.46–2.50)	0.027*
3rd	2.59 (1.66–3.55)	2.66 (1.69–3.69)	2.54 (1.58–3.41)	0.147
Increment	0.36 (−0.85 to 1.73)	0.37 (−0.86 to 1.73)	0.35 (−0.84 to 1.73)	0.775
$P^{\S}$	<0.001*	<0.001*	<0.001*	

Note: The designated plasma unit is ng/mL.
* P<0.05.
† The SPB group was contrasted with the control group.
§ Comparison between the first and third trimesters of pregnancy. Increment refers to the amount of Mo that increased from the first trimester to the third trimester.
Abbreviation: SPB=spontaneous preterm birth; Mo=molybdenum; IQR=interquartile range.

TABLE 3. Relationship between maternal molybdenum concentration and the risk of spontaneous premature birth.

Mo concentration	SPB	Control	Odds ratio (95% *CI*)					
			Model 1†	*P*	Model 2§	*P*	Model 3¶	*P*
Plasma 1st, *n* (%)								
<1.531	53 (22.46)	64 (27.12)	1		1		1	
1.531–2.074	59 (25.00)	60 (25.42)	1.179 (0.713, 1.950)	0.521	1.206 (0.714, 2.037)	0.485	1.217 (0.715, 2.072)	0.469
2.074–2.584	54 (22.88)	64 (27.12)	1.000 (0.604, 1.656)	1	1.031 (0.611, 1.739)	0.908	1.084 (0.635, 1.848)	0.768
≥2.584	70 (29.66)	48 (20.34)	1.878 (1.129, 3.124)	0.015*	1.892 (1.118, 3.201)	0.018*	2.074 (1.212, 3.550)	0.008*
P_{trend}			0.036*		0.039*		0.017*	
Plasma 3rd, *n* (%)								
<1.664	57 (24.15)	61 (25.96)	1		1		1	
1.664–2.593	55 (23.31)	62 (26.38)	0.968 (0.585, 1.600)	0.898	0.995 (0.590, 1.678)	0.984	0.977 (0.574, 1.665)	0.933
2.593–3.554	59 (25.00)	60 (25.53)	1.085 (0.656, 1.795)	0.750	1.129 (0.669,1.903)	0.649	1.132 (0.667, 1.923)	0.645
≥3.554	65 (27.54)	52 (22.13)	1.437 (0.868, 2.379)	0.159	1.570 (0.931, 2.649)	0.091	1.732 (1.016, 2.953)	0.044*
P_{trend}			0.140		0.079		0.038*	

Note: The designated plasma unit is ng/mL. In the Plasma 1st: SPB: *n*=236; Control: *n*=236; In the Plasma 3rd: SPB: *n*=236; Control: *n*=235.
Abbreviation: SPB=spontaneous preterm birth; Mo=molybdenum; *CI*=confidence interval; PPBMI=pre-pregnancy body mass index.
* P<0.05.
† Unconditional logistic regression with no adjustments.
§ Unconditional logistic regression with adjustments for maternal age, PPBMI, parity, and delivery way.
¶ Unconditional logistic regression with adjustments for maternal age, ethnicity, PPBMI, parity, delivery way, education, and income levels.

Fetal Growth Studies reported maternal plasma Mo concentration of 1.9 [interquartile range (IQR): 1.3] μg/L at 10–13 weeks gestation among 1,720 subjects (*6*). Yin et al. (*7*) reported Mo concentrations in the serum of pregnant women recorded as 2.378 (1.757–2.938) ng/mL, 2.413 (1.835–2.970) ng/mL, 2.327 (1.727–2.930) ng/mL, and 2.816 (2.392–3.496) ng/mL in cases of total orofacial clefts, cleft lip with cleft palate, cleft lip only (*n*=130), and in controls (*n*=260) respectively. These samples were collected at <28, 28–37, or ≥37 gestational weeks. In another study, maternal serum Mo levels were 2.51 (1.43–3.07) ng/mL and 2.66 (2.03–3.27) ng/mL in neural tube defects (NTDs) cases (*n*=273) and controls (*n*=477), respectively. These blood samples were collected at <28, 28–37, or ≥37 gestational weeks (*8*). Since Mo binds to α 2-macroglobulins in the form of molybdate, and spectrin on erythrocytes (*9*), it is expected that the Mo concentrations in plasma and serum would be nearly identical (*10*).

As a metal element, Mo is widely used in metallurgy, electronics, missiles and many other important areas (*11–13*). It is also found in everyday items like toys, clothing, as well as household and plant care products (*10*), suggesting an increased risk of exposure to Mo (*14*). The primary sources of Mo in humans are water and dietary intake. Foods rich in Mo include beans, wheat, oats, asparagus, milk, and cheese, with its

concentration in food varying based on the levels found in the local soil and water where the food was cultivated (*15*). Once absorbed, Mo is primarily localized in the kidneys, liver, and bones, with negligible levels crossing the placental barrier (*16–18*). Although Mo deficiencies are uncommon given their ultratrace occurrence, excessive consumption can result in health complications such as joint pain, hyperuricuria, hallucinations, and seizures (*19*). Moreover, Mo metabolism is closely linked with copper and sulfur metabolism. Excessive intake of molybdate can heighten the formation of copper sulfide, causing copper deficiency (*20–21*).

Certain limitations in our study merit attention. First, our participant pool came exclusively from Beijing, which should be considered when generalizing our findings to other regions. Furthermore, data collection did not include nutrient supplements or medication intake during pregnancy.

Our study reveals a preliminary correlation between maternal Mo levels and SPB risk, providing new insights into Mo's potential toxic effects on SPB. Currently, many regions in China lack reference ranges for trace element concentrations, and the risk of disease due to excessive trace elements is often overlooked by clinicians. Our findings emphasize the need for vigilant monitoring of Mo levels during pregnancy, particularly in Mo mining areas. Timely monitoring of trace element concentrations, such as Mo, in early pregnancy stages enables clinicians to intervene swiftly, thereby diminishing potential health risks to the mother and fetus. Going forward, comprehensive, nationwide multi-center studies that include dietary and nutritional surveys are needed to further investigate these issues.

Conflicts of interest: No conflicts of interest.

Funding: Supported by Beijing Hospitals Authority' Ascent Plan (DFL20191402), National Natural Science Foundation of China (82171671), Scientific Research Common Program of Beijing Municipal Commission of Education (KM202110025007), the National Key Research and Development Program of China (2016YFC1000304), and Beijing Natural Science Foundation (7222248).

doi: 10.46234/ccdcw2024.051

[#] Corresponding authors: Guanghui Li, liguanghui@ccmu.edu.cn; Zhiwen Li, lizw@bjmu.edu.cn.

[1] Division of Endocrinology and Metabolism, Department of Obstetrics, Beijing Obstetrics and Gynecology Hospital, Capital Medical University. Beijing Maternal and Child Health Care Hospital, Beijing, China; [2] Department of Obstetrics and Gynecology, Beijing Luhe Hospital, Capital Medical University, Beijing, China; [3] Institute of Reproductive and Child Health, National Health Commission Key Laboratory of Reproductive Health, Peking University, Beijing, China; [4] Department of Epidemiology and Biostatistics, School of Public Health, Peking University, Beijing, China; [5] Department of Laboratorial Science and Technology, School of Public Health, Peking University, Beijing, China.

Submitted: December 27, 2023; Accepted: February 21, 2024

REFERENCES

1. Cobo T, Kacerovsky M, Jacobsson B. Risk factors for spontaneous preterm delivery. Int J Gynaecol Obstet 2020;150(1):17 – 23. https://doi.org/10.1002/ijgo.13184.
2. Walani SR. Global burden of preterm birth. Int J Gynecol Obstet 2020;150(1):31 – 3. https://doi.org/10.1002/ijgo.13195.
3. Howe CG, Margetaki K, Vafeiadi M, Roumeliotaki T, Karachaliou M, Kogevinas M, et al. Prenatal metal mixtures and child blood pressure in the Rhea mother-child cohort in Greece. Environ Health 2021;20(1):1. https://doi.org/10.1186/s12940-020-00685-9.
4. Zhao H, Wu WJ, Zhang X, Zhu QH, Tang J, He HS, et al. Associations between molybdenum exposure and ultrasound measures of fetal growth parameters: a pilot study. Chemosphere 2021;269:128709. https://doi.org/10.1016/j.chemosphere.2020.128709.
5. Karakis I, Landau D, Gat R, Shemesh N, Tirosh O, Yitshak-Sade M, et al. Maternal metal concentration during gestation and pediatric morbidity in children: an exploratory analysis. Environ Health Prev Med 2021;26(1):40. https://doi.org/10.1186/s12199-021-00963-z.
6. Zheng YN, Zhang CL, Weisskopf MG, Williams PL, Claus Henn B, Parsons PJ, et al. Evaluating associations between early pregnancy trace elements mixture and 2nd trimester gestational glucose levels: a comparison of three statistical approaches. Int J Hyg Environ Health 2020;224:113446. https://doi.org/10.1016/j.ijheh.2019.113446.
7. Yin SJ, Wang CR, Wei J, Jin L, Liu JF, Wang LL, et al. Selected essential trace elements in maternal serum and risk for fetal orofacial clefts. Sci Total Environ 2020;712:136542. https://doi.org/10.1016/j.scitotenv.2020.136542.
8. Tian T, Yin SJ, Jin L, Liu JF, Wang CR, Wei J, et al. Single and mixed effects of metallic elements in maternal serum during pregnancy on risk for fetal neural tube defects: a Bayesian kernel regression approach. Environ Pollut 2021;285:117203. https://doi.org/10.1016/j.envpol.2021.117203.
9. Schultze B, Lind PM, Larsson A, Lind L. Whole blood and serum concentrations of metals in a Swedish population-based sample. Scand J Clin Lab Invest 2014;74(2):143 – 8. https://doi.org/10.3109/00365513.2013.864785.
10. Hays SM, Macey K, Poddalgoda D, Lu M, Nong A, Aylward LL. Biomonitoring Equivalents for molybdenum. Regul Toxicol Pharmacol 2016;77:223 – 9. https://doi.org/10.1016/j.yrtph.2016.03.004.
11. Abernethy DR, DeStefano AJ, Cecil TL, Zaidi K, Williams RL, USP Metal Impurities Advisory Panel. Metal impurities in food and drugs. Pharm Res 2010;27(5):750 – 5. https://doi.org/10.1007/s11095-010-0080-3.
12. Gracco A, Dandrea M, Deflorian F, Zanella C, De Stefani A, Bruno G, et al. Application of a molybdenum and tungsten disulfide coating to improve tribological properties of orthodontic archwires. Nanomaterials 2019;9(5):753. https://doi.org/10.3390/nano9050753.
13. Kwinta P, Pietrzyk JJ. Preterm birth and respiratory disease in later life. Expert Rev Respir Med 2010;4(5):593 – 604. https://doi.org/10.1586/ers.10.59.
14. Gao L, Gao B, Peng WQ, Xu DY, Yin SH. Assessing potential release tendency of As, Mo and W in the tributary sediments of the Three Gorges Reservoir, China. Ecotoxicol Environ Saf 2018;147:342 – 8. https://doi.org/10.1016/j.ecoenv.2017.08.036.
15. Novotny JA, Peterson CA. Molybdenum. Adv Nutr 2018;9(3):272 – 3. https://doi.org/10.1093/advances/nmx001.

16. Rosoff B, Spencer H. The distribution and excretion of molybdenum-99 in mice. Health Phys 1973;25(2):173-5. https://pubmed.ncbi.nlm.nih.gov/4784249/.
17. Bremner I. The toxicity of cadmium, zinc and molybdenum and their effects on copper metabolism. Proc Nutr Soc 1979;38(2):235 – 42. https://doi.org/10.1079/pns19790037.
18. Shirley RL, Jeter MA, Feaster JP, McCall JT, Outler JC, Davis GK. Placental transfer of Mo^{99} and Ca^{45} in swine. J Nutr 1954;54(1):59 – 64. https://doi.org/10.1093/jn/54.1.59.
19. Neve J. The nutritional importance and physiopathology of molybdenum in man. J Pharm Belg 1991;46(3):189-96. https://pubmed.ncbi.nlm.nih.gov/1757880/.
20. Mason J. Thiomolybdates: mediators of molybdenum toxicity and enzyme inhibitors. Toxicology 1986;42(2-3):99 – 109. https://doi.org/10.1016/0300-483x(86)90001-6.
21. Seelig MS. Proposed ce: role of copper-molybdenum interaction in iron-deficiency and iron-storage diseases. Am J Clin Nutr 1973;26(6):657 – 72. https://doi.org/10.1093/ajcn/26.6.657.

SUPPLEMENTARY MATERIAL

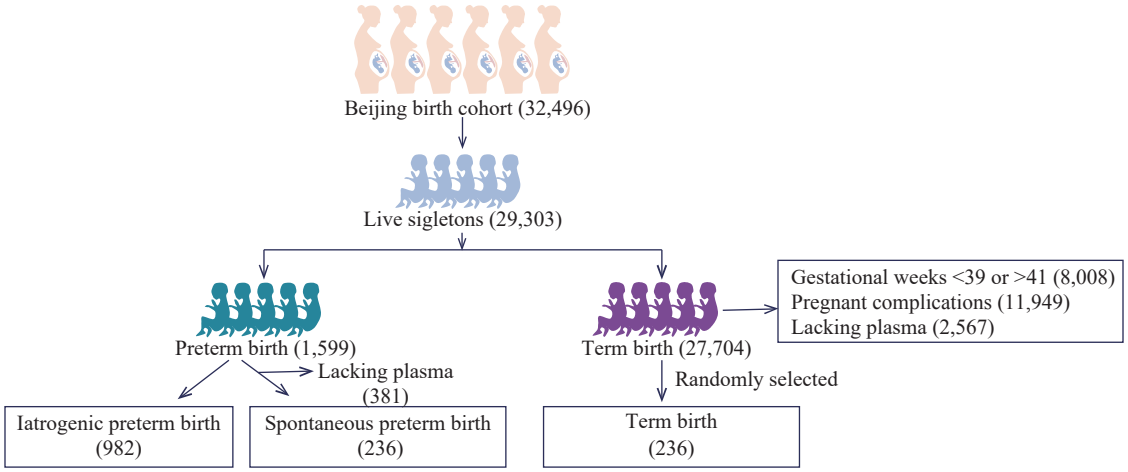

SUPPLEMENTARY FIGURE S1. Flow chart illustrating the selection of cases and controls.

SUPPLEMENTARY TABLE S1. Association between maternal plasma molybdenum concentration and the risk of spontaneous preterm birth at varying pre-pregnancy body mass indexes.

PPBMI levels	Odds ratio (95% *CI*)					
	Model 1[†]	*P*	Model 2[§]	*P*	Model 3[¶]	*P*
1st						
<18.5	1.995 (1.007, 3.952)	0.048*	1.855 (0.926, 3.716)	0.081	2.076 (0.853, 5.053)	0.107
18.5–25	1.200 (0.971, 1.483)	0.092	1.203 (0.972, 1.489)	0.090	1.237 (0.994, 1.541)	0.057
≥25	1.529 (0.854, 2.736)	0.153	1.633 (0.899, 2.967)	0.107	2.698 (1.209, 6.020)	0.015*
3rd						
<18.5	1.182 (0.775, 1.804)	0.437	1.174 (0.753, 1.831)	0.479	1.348 (0.790, 2.299)	0.274
18.5–25	1.161 (0.980, 1.374)	0.084	1.190 (1.002, 1.414)	0.048*	1.200 (1.007, 1.431)	0.042*
≥25	0.909 (0.561, 1.473)	0.698	0.900 (0.553, 1.465)	0.672	0.944 (0.514, 1.734)	0.853

Abbreviation: SPB=spontaneous preterm birth; Mo=molybdenum; *CI*=confidence interval; PPBMI=pre-pregnancy body mass index.
* *P*<0.05.
[†] Unconditional logistic regression with no adjustments.
[§] Unconditional logistic regression with adjustments for maternal age, parity, and delivery way.
[¶] Unconditional logistic regression with adjustments for maternal age, ethnicity, parity, delivery way, education, and income levels.

SUPPLEMENTARY TABLE S2. Association between maternal plasma molybdenum concentration and the risk of spontaneous preterm birth at varying parity levels.

Parity	Odds ratio (95% *CI*)					
	Model 1[†]	*P*	Model 2[§]	*P*	Model 3[¶]	*P*
1st						
0	1.185 (0.957, 1.467)	0.119	1.173 (0.946, 1.454)	0.146	1.219 (0.976, 1.523)	0.080
≥1	1.762 (1.144, 2.713)	0.010*	1.755 (1.124, 2.740)	0.013*	2.271 (1.315, 3.921)	0.003*
3rd						
0	1.189 (0.996, 1.419)	0.055	1.194 (0.997, 1.430)	0.054	1.204 (1.002, 1.445)	0.047*
≥1	1.104 (0.837, 1.456)	0.485	1.108 (0.832, 1.476)	0.482	1.117 (0.813, 1.533)	0.496

Abbreviation: SPB=spontaneous preterm birth; Mo=molybdenum; *CI*=confidence interval; PPBMI=pre-pregnancy body mass index.
* *P*<0.05.
[†] Unconditional logistic regression without any adjustments.
[§] Implementation of unconditional logistic regression adjustments considering variables such as maternal age, PPBMI, and mode of delivery.
[¶] Unconditional logistic regression was utilized, accounting for variables including maternal age, ethnicity, PPBMI, mode of delivery, educational attainment, and income brackets.

SUPPLEMENTARY TABLE S3. Association between maternal Mo concentration and SPB in the sensitivity analysis.

Mo concentration	SPB	Control	Odds ratio (95% *CI*)					
			Model 1[†]	*P*	Model 2[§]	*P*	Model 3[¶]	*P*
Plasma 1st								
<1.529	48 (21.92%)	61 (27.98%)	1		1		1	
1.529–2.070	56 (25.57%)	54 (24.77%)	1.280 (0.760, 2.156)	0.353	1.329 (0.781, 2.261)	0.295	1.379 (0.802, 2.370)	0.246
2.070–2.571	49 (22.37%)	60 (27.52%)	1.074 (0.637, 1.810)	0.790	1.127 (0.660, 1.925)	0.661	1.204 (0.698, 2.076)	0.505
≥2.571	66 (30.14%)	43 (19.73%)	2.024 (1.189, 3.445)	0.009*	2.105 (1.225, 3.620)	0.007*	2.235 (1.286, 3.885)	0.004*
P_{trend}			0.025*		0.018*		0.011*	
Plasma 3rd								
<1.692	56 (25.57%)	53 (24.42%)	1		1		1	
1.692–2.612	49 (22.37%)	60 (27.65%)	0.868 (0.514, 1.467)	0.597	0.880 (0.512, 1.511)	0.642	0.885 (0.511, 1.532)	0.662
2.612–3.558	55 (25.11%)	54 (24.88%)	1.018 (0.604, 1.717)	0.946	1.038 (0.606, 1.777)	0.892	1.131 (0.597, 1.778)	0.914
≥3.558	59 (26.95%)	50 (23.05%)	1.258 (0.745, 2.124)	0.391	1.421 (0.772, 2260)	0.310	1.686 (1.003, 2.794)	0.048*
P_{trend}			0.313		0.245		0.041*	

Note: The unit used is ng/mL. Excluded: Vaginal infection cases involving group B streptococcus, fungal, and mycoplasma infections were not included in both the SPB group (*n*=17) and the TB group (*n*=18). In the first plasma group: SPB: *n*=219; Control: *n*=218. In the third plasma group: SPB: *n*=219; Control: *n*=217.

Abbreviation: SPB=spontaneous preterm birth; Mo=molybdenum; *CI*=confidence interval; PPBMI=pre-pregnancy body mass index.

* *P*<0.05.

[†] Unconditional logistic regression without any adjustments.

[§] Unconditional logistic regression was performed, adjusting for factors such as maternal age, PPBMI, parity, and mode of delivery.

[¶] Unconditional logistic regression was utilized, while controlling for factors such as maternal age, ethnicity, pre-pregnancy body mass index, parity, method of delivery, educational attainment, and income levels.

Vital Surveillances

The Relationship Between the Atmospheric Environment and Road Traffic Fatalities — Shandong Province, China, 2012–2021

Tao Wang[1]; Jie Chu[2]; Zhiying Yao[1]; Li Yang[1]; Zilong Lu[2]; Ge Tian[1]; Xiaolei Guo[2,#]; Cunxian Jia[1,#]

ABSTRACT

Introduction: This study aims to analyze the potential impact of the meteorological environment and air pollutants on road traffic fatalities.

Methods: Road traffic fatality data in Shandong Province from 2012 to 2021 were obtained from the Population Death Information Registration Management System. Meteorological and air pollutant data for the same period were collected from the U.S. National Oceanic and Atmospheric Administration and the Ecological Environment Monitoring Center of Shandong Province, China. Pearson's correlation and ridge regression were used to analyze the impact of the meteorological environment and air pollutants on road traffic fatalities.

Results: From 2012 to 2021, there were 163,863 road traffic fatality cases. The results of the ridge regression analysis showed that the daily average temperature was negatively correlated with total fatalities and passengers and positively correlated with pedestrians, nonmotorized drivers, and motorized drivers. The daily minimum temperature was negatively correlated with total fatalities and positively correlated with motorized drivers. The daily maximum temperature was positively correlated with both pedestrian and nonmotorized drivers. The daily accumulated precipitation was negatively correlated with pedestrians. Sunshine duration was positively correlated with both nonmotorized and motorized drivers. Inhalable particulate matter (PM_{10}) and nitrogen dioxide (NO_2) were positively correlated with total fatalities, pedestrians, and nonmotorized drivers. Sulfur dioxide (SO_2) was positively correlated with total fatalities but negatively correlated with nonmotorized drivers, passengers, and motorized drivers.

Conclusions: Atmospheric factors associated with the occurrence of road traffic fatalities include air temperature, daily accumulated precipitation, sunshine duration, and air pollutants such as PM_{10}, NO_2, and SO_2.

Road traffic accidents are incidents that occur on a road or highway and involve at least one moving vehicle, resulting in injuries, property damage, or loss of life (*1*). The current global annual death toll from road traffic accidents is approximately 1.3 million people. Moreover, road traffic accidents have emerged as the primary cause of death for children and young adults globally (*2*). Road traffic accidents in China result in more than 250,000 deaths annually, accounting for approximately 19% of the total deaths worldwide(*3*). Investigating the potential factors influencing road traffic accidents is essential for reducing and preventing them.

Road traffic accidents involve three elements: humans, vehicles, and the environment. Meteorological conditions, including sunshine duration, precipitation, and high temperatures, contribute to road traffic accidents (*4*). Meteorological conditions directly impact the friction between vehicle tires and the road surface while also indirectly influencing drivers' emotions, perceptions, and behavior (*5*). Although it may seem that there is no relationship between air pollution and traffic accidents, haze caused by air pollution reduces visibility, which can lead to limited visibility. Moreover, air pollutants can cause both immediate injuries and long-term hazards to human health. Previous research (*6*) has suggested that air pollutants directly stimulate drivers' eyes, resulting in redness and pain, as well as headaches due to long-term effects. Therefore, exploring the impact of the meteorological environment and air pollutants on road traffic fatalities is critical for reducing road traffic accidents.

METHODS

Data on road traffic fatalities in Shandong Province were obtained from the Population Death Information Registration Management System of the Chinese Centers for Disease Control and Prevention during the period of death from January 2012 to December 2021. According to the cause of death classification and coding range of the International Classification of Diseases 10th Revision (ICD-10) in the Technical Guidance for Reporting Cause of Death, road traffic accident data that were included in the analysis were divided into four subgroups: pedestrian, nonmotorized driver, passenger, and motorized driver.

The atmospheric environmental data were divided into two parts: meteorological data and air pollution data.

The meteorological data of Shandong Province were obtained from the National Centers for Environmental Information (NCEI), which is part of the National Oceanic and Atmospheric Administration (NOAA) (http://www.ncei.noaa.gov) in the U.S from January 2012 to December 2021. The meteorological data consist of the following parameters: daily average temperature, daily maximum temperature, daily minimum temperature, maximum wind speed, relative humidity, daily accumulated precipitation, and sunshine duration.

The air pollution data were obtained from the Ecological Environment Monitoring Center of Shandong Province, China (http://www.sdem.org.cn/), from January 2012 to December 2021. The air pollutant data include the air quality index (AQI), fine particulate matter ($PM_{2.5}$), inhalable particulate matter (PM_{10}), sulfur dioxide (SO_2), nitrogen dioxide (NO_2), ozone (O_3), and carbon monoxide (CO).

R software (version 4.3.1; R Core Team, Vienna, Austria) was used for statistical analysis. We employed Pearson's correlation analysis to investigate the association between road traffic fatalities and the atmospheric environment. Ridge regression analysis was used to investigate the influence of the atmospheric environment on road traffic fatalities while accounting for multicollinearity. The minimum k value, which occurs when the standardized regression coefficients of each variable tend to stabilize, was chosen as the model's k value selection principle. The significance level of α was 0.05.

RESULTS

From 2012 to 2021, there were 163,863 road traffic fatality cases in Shandong Province. The mean age of individuals involved in road traffic fatalities was 51.97 years [standard deviation (SD): 18.10 years]. The findings indicated a positive correlation between daily average temperature and daily maximum temperature and total fatalities and each subgroup. The daily minimum temperature and sunshine duration were positively correlated with total fatalities and associated subgroups, except for pedestrians. The daily accumulated precipitation exhibited negative correlations with total fatalities and pedestrians. There was a positive correlation between relative humidity and pedestrians, but no association was found with total fatalities or other subgroups (Table 1).

There were associations between the AQI and total fatalities and the fatality subgroups. Specifically, the AQI was negatively associated with motorized drivers and positively associated with both total fatalities and the remaining subgroups. Further analysis revealed that PM_{10}, SO_2 and CO were positively correlated with pedestrians, nonmotorized drivers, and passengers and negatively correlated with motorized drivers. NO_2 was

TABLE 1. Correlations between meteorological conditions and road traffic fatalities in Shandong Province, China, 2012–2021.

Variable	Total (N=163,863)	Pedestrian (n_1=90,726)	Nonmotorized driver (n_2=23,730)	Passenger (n_3=14,339)	Motorized driver (n_4=35,068)
Maximum wind speed	−0.095*	−0.093*	−0.051*	−0.036*	−0.022*
Daily average temperature	0.048*	0.018*	0.038*	0.016*	0.047*
Daily minimum temperature	0.034*	0.002	0.032*	0.013*	0.047*
Daily maximum temperature	0.057*	0.026*	0.043*	0.019*	0.047*
Daily accumulated precipitation	−0.019*	−0.021*	−0.004	0.000	−0.004
Sunshine duration	0.016*	−0.005	0.014*	0.012*	0.031*
Relative humidity	0.007	0.012*	0.006	−0.005	−0.004

* P<0.05.

TABLE 2. Correlations between air pollutants and road traffic fatalities in Shandong Province, China, 2012–2021.

Variable	Total (*N*=163,863)	Pedestrian (n_1=90,726)	Nonmotorized driver (n_2=23,730)	Passenger (n_3=14,339)	Motorized driver (n_4=35,068)
AQI	0.097*	0.124*	0.016*	0.035*	−0.021*
$PM_{2.5}$ (μg/m^3)	0.077*	0.110*	0.006	0.033*	−0.034*
PM_{10} (μg/m^3)	0.112*	0.135*	0.024*	0.044*	−0.010*
SO_2 (μg/m^3)	0.063*	0.095*	−0.024*	0.046*	−0.026*
NO_2 (μg/m^3)	0.112*	0.116*	0.036*	0.049*	0.019*
O_3 (μg/m^3)	0.008	−0.014*	0.017*	−0.009	0.036*
CO (mg/m^3)	0.089*	0.125*	0.013*	0.046*	−0.042*

Abbrevitation: AQI=air quality index; $PM_{2.5}$=fine particulate matter; PM_{10}=inhalable particulate matter; SO_2=sulfur dioxide; NO_2=nitrogen dioxide; O_3=ozone; CO=carbon monoxide.
* P<0.05.

positively associated with both total fatalities and fatality subgroups. There was a positive correlation between O_3 and both nonmotorized and motorized drivers and a negative correlation between O_3 and pedestrians (Table 2).

The ridge regression analysis included variables in the atmosphere that were correlated with total road traffic fatalities and associated variables. For total fatalities, the ridge regression model yielded a k value of 0.198 and an F value of 9.638 (P<0.001), indicating the statistical significance of the model. The results showed that maximum wind speed (β=−0.030, P<0.001), daily average temperature (β=−0.009, P<0.001), daily minimum temperature (β=−0.007, P=0.021), and $PM_{2.5}$ (β=−0.021, P<0.001) were negatively correlated with total fatalities, whereas PM_{10} (β=0.019, P<0.001), SO_2 (β=0.009, P=0.046), and NO_2 (β=0.010, P=0.036) were positively correlated. For pedestrians, the ridge regression model yielded a k value of 0.195 and an F value of 64.389 (P<0.001), indicating the statistical significance of the model.

The maximum wind speed (β=−0.054, P<0.001), daily accumulated precipitation (β=-0.010, P=0.017), and O_3 (β=−0.030, P<0.001) were negatively correlated with pedestrians. Conversely, daily average temperature (β=0.014, P<0.001), daily maximum temperature (β=0.034, P<0.001), relative humidity (β=0.013, P=0.003), PM_{10} (β=0.069, P<0.001), NO_2 (β=0.021, P<0.001), and CO (β=0.015, P<0.001) were positively correlated with pedestrians. For nonmotorized drivers, the ridge regression model yielded a k value of 0.183 and an F value of 38.579 (P<0.001), indicating the statistical significance of the model. There were negative correlations with maximum wind speed (β=−0.035, P<0.001), SO_2 (β=−0.038, P<0.001), and O_3 (β=−0.028, P<0.001), while positive correlations were observed with daily average temperature (β=0.022, P<0.001), daily maximum temperature (β=0.035, P<0.001), sunshine duration (β=0.014, P=0.001), PM_{10} (β=0.013, P=0.005), and NO_2 (β=0.056, P<0.001). For passengers, the ridge regression model yielded a k value of 0.200 and an F value of 2.919 (P=0.001), indicating the statistical significance of the model. There were negative correlations between the daily average temperature (β=−0.006, P=0.002), SO_2 (β=−0.015, P=0.001), and NO_2 (β=−0.011, P=0.024) and passengers. The ridge regression model for motorized drivers had a k value of 0.195 and an F value of 15.868 (P<0.001), indicating the statistical significance of the model. There were positive correlations with daily average temperature (β=0.010, P<0.001), daily minimum temperature (β=0.024, P<0.001), sunshine duration (β=0.013, P=0.002), and NO_2 (β=0.045, P<0.001), while there was a negative correlation with SO_2 (β=−0.019, P<0.001) (Table 3).

DISCUSSION

From 2012 to 2021, there were a large number of road traffic fatalities in Shandong Province, China. Atmospheric conditions were correlated with road traffic fatalities, air temperature, daily accumulated precipitation, sunshine duration, PM_{10}, SO_2, and NO_2 were positively or negatively correlated with total road traffic fatalities and each subgroup.

Multiple atmospheric factors were found to be correlated with road traffic fatalities. The maximum wind speed was negatively correlated with pedestrian and nonmotorized driver speeds, similar findings to those of Gao et al. (*7*). Pedestrians and nonmotorized drivers often refrain from traveling or choose alternative modes of transport under high winds due to their light weight and inadequate wind resistance.

TABLE 3. Ridge regression analysis of the atmospheric environment and road traffic fatalities in Shandong Province, China, 2012–2021.

Variable	Total			Pedestrian			Nonmotorized driver			Passenger			Motorized driver		
	β	*t*	*P*	*β*	*t*	*P*	*β*	*t*	*P*	*β*	*t*	*P*	*β*	*t*	*P*
Intercept		84.706	<0.001		52.112	<0.001		92.243	<0.001		198.917	<0.001		143.573	<0.001
Maximum wind speed	−0.030	−7.252	<0.001	−0.054	−12.791	<0.001	−0.035	−8.321	<0.001	0.002	0.419	0.675	−0.006	−1.380	0.168
Daily average temperature	−0.009	−4.408	<0.001	0.014	4.497	<0.001	0.022	−9.549	<0.001	−0.006	−3.104	0.002	0.010	4.608	<0.001
Daily minimum temperature	−0.007	−2.309	0.021				0.006	1.708	0.088	−0.005	−1.787	0.074	0.024	7.725	<0.001
Daily maximum temperature	0.002	0.678	0.498	0.034	10.876	<0.001	0.035	10.976	<0.001	−0.002	−0.782	0.434	0.005	1.608	0.108
Daily accumulated precipitation	0.006	1.348	0.178	−0.010	−2.38	0.017									
Sunshine duration	−0.005	−1.086	0.278				0.014	3.310	0.001	0	−0.098	0.922	0.013	3.148	0.002
Relative humidity				0.013	2.942	0.003									
$PM_{2.5}$ (μg/m^3)	−0.021	−4.743	<0.001	−0.008	−1.820	0.069				0.008	1.788	0.074	−0.030	−6.732	<0.001
PM_{10} (μg/m^3)	0.019	4.175	<0.001	0.069	15.700	<0.001	0.013	2.784	0.005	0	−0.079	0.937	0.009	1.915	0.056
SO_2 (μg/m^3)	0.009	1.998	0.046	0.001	0.231	0.818	−0.038	−7.979	<0.001	−0.015	−3.256	0.001	−0.019	−4.017	<0.001
NO_2 (μg/m^3)	0.010	2.093	0.036	0.021	4.296	<0.001	0.056	11.400	<0.001	−0.011	−2.265	0.024	0.045	9.032	<0.001
O_3 (μg/m^3)				−0.030	−6.446	<0.001	−0.028	−5.741	<0.001				−0.006	−1.135	0.256
CO (mg/m^3)	0.001	0.267	0.790	0.015	3.499	<0.001	−0.003	−0.737	0.461	−0.006	−1.448	0.147	−0.008	−1.829	0.067

Abbrevitation: AQI=air quality index; $PM_{2.5}$=fine particulate matter; PM_{10}=inhalable particulate matter; SO_2=sulfur dioxide; NO_2=nitrogen dioxide; O_3=ozone; CO=carbon monoxide.

Temperature was also associated with road traffic fatalities. There was a positive correlation between daily minimum temperature and road traffic fatalities, affecting motorized drivers. Low temperatures may cause icy road surfaces, leading to tire skidding and consequently increasing the risk of traffic accidents. High temperatures can also contribute to an increase in road traffic fatalities. High temperatures can alter the physical properties of vehicle tires (*8*), resulting in modified vehicle performance and posing risks to safe driving behavior. Li et al. (*9*) demonstrated that precipitation, particularly extreme precipitation, increases the risk of road traffic accidents. In this study, precipitation was found to be negatively correlated only with road traffic fatalities involving pedestrians. Precipitation can make travel inconvenient, particularly for pedestrians. Therefore, during precipitation events, pedestrians tend to venture outdoors less frequently, consequently reducing the risk of accidents in vulnerable traffic conditions.

In this study, several air pollutants that were significantly correlated with total road traffic fatalities and specific subgroups were identified. PM_{10} exhibited positive correlations with road traffic fatalities involving pedestrians and nonmotorized drivers. Particulate matter decreases atmospheric visibility (*10*), increasing the likelihood of traffic accidents due to limited driver visibility. Particulate matter, which frequently includes heavy metals, can impact a driver's visual and olfactory senses (*11*), ultimately affecting the driver's behavior behind the wheel.

This study revealed that there was a positive correlation between NO_2 concentration and road traffic fatalities. Nitrogen oxides (NO_x), which originate mainly from motor vehicle exhaust, are the primary pollutants responsible for the formation of photochemical smog. Photochemical smog is a potent irritant that causes acute effects on the human eye and respiratory tract, resulting in allergic reactions, including tearing, sneezing, and coughing. In addition, NO_x can have psychological and cognitive impacts on drivers (*12*). Both the acute and long-term effects of NO_x can significantly harm the human body, particularly drivers, and pose substantial risks to traffic safety.

The atmospheric data used in this study correspond to the day of the fatality rather than the atmospheric conditions during the traffic accident, and the atmospheric conditions may also have a lag effect on road traffic fatalities, which may result in misleading associations. A study demonstrated (*13*) that approximately 60% of individuals do not survive beyond the first hour of a road traffic accident, indicating a high rate of timely mortality. Additionally,

the current study was an ecological study, and individual information on road traffic fatalities, particularly regarding unsafe driving behavior, was not collected. In the future, a survey will be conducted to collect individual information on road traffic fatalities in Shandong Province, aiming to analyze the contributing factors to road traffic fatalities comprehensively. This study is based on an analysis of the cause of death and atmospheric monitoring, which has positive implications for the prevention of road traffic fatalities and the development of related policies.

The occurrence of road traffic fatalities was found to be linked to meteorological factors, including air temperature; daily accumulated precipitation, and air pollutants such as particulate matter and NO_2. The implementation of atmospheric environmental management to reduce air pollution levels, as well as timely and accurate weather warnings and forecasts, has a positive impact on reducing the incidence of road traffic fatalities.

Conflicts of interest: No conflicts of interest.

doi: 10.46234/ccdcw2024.052

[#] Corresponding authors: Xiaolei Guo, guoxiaolei@126.com; Cunxian Jia, jiacunxian@sdu.edu.cn.

[1] Department of Epidemiology, School of Public Health, Cheeloo College of Medicine, Shandong University, Jinan, Shandong Province, China; [2] Department for Chronic and Non-Communicable Disease Control and Prevention, Shandong Center for Disease Control and Prevention, Jinan, Shandong Province, China.

Submitted: November 16, 2023; Accepted: February 29, 2024

REFERENCES

1. Ma XL. Thematic analysis of tort civil liability for road traffic accidents. Beijing: China University of Political Science and Law Press. 2018; p. 3-4. https://book.kongfz.com/181694/6226319591/. (In Chinese).
2. World Health Organization. Global status report on road safety 2018. https://www.who.int/publications/i/item/9789241565684. [2023-10-10].
3. Yang TF, Zeng HT, Yang XA, Kong JW, Chen XZ, Zhou N, et al. Characteristics of road traffic accident types and casualties in Guangzhou, China, from 2007 to 2020: a retrospective cohort study based on the general population. Heliyon 2023;9(1):e12822. https://doi.org/10.1016/j.heliyon.2023.e12822.
4. Liang MM, Zhao DD, Wu YL, Ye PP, Wang Y, Yao ZH, et al. Short-term effects of ambient temperature and road traffic accident injuries in Dalian, Northern China: a distributed lag non-linear analysis. Accid Anal Prev 2021;153:106057. https://doi.org/10.1016/j.aap.2021.106057.
5. Fountas G, Sarwar T, Anastasopoulos PC, Blatt A, Majka K. Analysis of stationary and dynamic factors affecting highway accident occurrence: a dynamic correlated grouped random parameters binary logit approach. Accid Anal Prev 2018;113:330 – 40. https://doi.org/10.1016/j.aap.2017.05.018.
6. Gupta SK, Elumalai SP. Exposure to traffic-related particulate matter and deposition dose to auto rickshaw driver in Dhanbad, India. Atmos Pollut Res 2019;10(4):1128 – 39. https://doi.org/10.1016/j.apr.2019.01.018.
7. Gao JH, Chen XJ, Woodward A, Liu XB, Wu HX, Lu YG, et al. The association between meteorological factors and road traffic injuries: a case analysis from Shantou city, China. Sci Rep 2016;6:37300. https://doi.org/10.1038/srep37300.
8. Liang MM, Min M, Guo XW, Song QX, Wang H, Li N, et al. The relationship between ambient temperatures and road traffic injuries: a systematic review and meta-analysis. Environ Sci Pollut Res 2022;29(33):50647 – 60. https://doi.org/10.1007/s11356-022-19437-y.
9. Li DZ, Zhu XW, Huang GY, Feng HB, Zhu SY, Li X. A hybrid method for evaluating the resilience of urban road traffic network under flood disaster: an example of Nanjing, China. Environ Sci Pollut Res 2022;29(30):46306 – 24. https://doi.org/10.1007/s11356-022-19142-w.
10. Bilal M, Hassan M, Tahir DBT, Iqbal MS, Shahid I. Understanding the role of atmospheric circulations and dispersion of air pollution associated with extreme smog events over South Asian megacity. Environ Monit Assess 2022;194(2):82. https://doi.org/10.1007/s10661-021-09674-y.
11. Barthwal V, Jain S, Babuta A, Jamir C, Sharma AK, Mohan A. Health impact assessment of Delhi's outdoor workers exposed to air pollution and extreme weather events: an integrated epidemiology approach. Environ Sci Pollut Res 2022;29(29):44746 – 58. https://doi.org/10.1007/s11356-022-18886-9.
12. Li JJ, Zhang W. Research progress on the relationship between air pollution and cognitive impairment and its mechanism. Chin J Neuroimmunol Neurol 2020;27(2):151 – 4. https://doi.org/10.3969/j.issn.1006-2963.2020.015.
13. Wang TB, Wang YH, Xu TM, Li LB, Huo ML, Li X, et al. Epidemiological and clinical characteristics of 3327 cases of traffic trauma deaths in Beijing from 2008 to 2017: a retrospective analysis. Medicine 2020;99(1):e18567. https://doi.org/10.1097/MD.0000000000018567.

Vital Surveillances

Analysis and Monitoring of Indoor Radon Concentrations of 37 Kindergartens — Beijing Municipality, China, 2023

Meinan Yao[1]; Kuke Ding[2]; Xiaozhe Tang[2]; Yunyun Wu[3]; Yanchao Song[3]; Shuyuan Liu[3]; Bin Bai[1]; Li Zhang[2,#]; Yongzhong Ma[1,#]

ABSTRACT

Introduction: Radon (^{222}Rn or ^{222}radon) is a radioactive gas emitted from building materials, foundations, and soil. Children are especially susceptible to radon exposure, underscoring the need to assess indoor radon levels in kindergartens. This study monitored radon concentrations in 37 Beijing kindergartens from June to October 2023.

Methods: A random sample of 37 kindergartens was selected from 18 administrative districts in Beijing. The indoor radon concentration was measured using the solid track accumulation method, with radon detectors continuously monitored over a 3-month period.

Results: The mean indoor radon level in 37 kindergartens, observed at 252 monitoring points, was 84.3 Bq/m^3, with values varying from 12.9 to 263.5 Bq/m^3. About 20.2% of points showed radon levels between 100.0 and 200.0 Bq/m^3, while 2.4% exceeded 200.0 Bq/m^3. Notably, radon levels were significantly elevated on the ground floor compared to the upper floors.

Conclusion: Indoor radon levels in 37 kindergartens remained below the national standard limit of 300.0 Bq/m^3 for buildings (GB/T 16146-2015). Nonetheless, 18.9% of the kindergartens exceeded the 100.0 Bq/m^3 limit set for new constructions. It is advised to improve radon monitoring in kindergartens and consider developing a national standard for maximum permissible radon levels in such facilities.

Radon (^{222}Rn or ^{222}radon) is a naturally occurring radioactive gas that is both colorless and odorless. It is frequently encountered in human living environments, predominantly as ^{222}Rn. The International Agency for Research on Cancer (IARC) has classified radon as a Group 1 carcinogen, indicating its well-established cancer-causing properties. Additionally, the World Health Organization (WHO) has identified radon as one of 19 recognized carcinogens. Statistical evidence demonstrates that exposure to radon is the second leading cause of lung cancer, following tobacco smoking (*1*).

The critical need to address indoor radon exposure in educational settings for young children is underscored by their increased susceptibility to the adverse effects of this radiation. Due to their rapid physiological development and less mature immune systems, young children are particularly vulnerable to indoor radon and its decay products. Furthermore, when normalized for body weight, the respiratory rates of young children are 50% greater than those of adults (*2*), enhancing their risk when exposed to elevated radon levels in indoor environments. Consequently, the potential harm to both the physical and cognitive development of children from indoor radon radiation demands heightened scrutiny and intervention.

In 1988, the IARC classified radon as a known human carcinogen. Responding to the escalating concerns over radon's health risks, the Indoor Radon Abatement Act was enacted to lower indoor radon concentrations nationwide to match outdoor levels (*3*). Additionally, the International Commission on Radiological Protection (ICRP) publication 126 (2014) recommended monitoring indoor radon levels in kindergarten facilities as a part of broader radon surveillance measures. It emphasized the importance of preventing and reducing radon exposure in public spaces like kindergartens (*4*).

In order to investigate indoor radon levels in kindergartens and contribute to the establishment of monitoring and prevention guidelines, a study was carried out in Beijing. Thirty-seven kindergartens in 18 administrative districts were chosen, and indoor radon levels were monitored from June to October 2023. The objective was to assess the prevailing indoor radon concentrations in kindergartens throughout the city.

METHODS

Beijing is comprised of 18 districts. To achieve representative surveillance, 37 kindergartens were selected through random sampling. Within these kindergartens, surveillance points were designated in various locations, including sleeping quarters, play areas, and administrative offices, resulting in a total of 252 surveillance points. These points provided extensive coverage of the environments frequented by the kindergarten staff and children. As per our conceptualized monitoring strategy, we deployed a cumulative detector at each surveillance point. In order to obtain precise data, these detectors were strategically placed no less than 30 centimeters from any wall and positioned away from zones with direct airflow, such as those near doors, windows, and air conditioning units.

The indoor radon concentration at each monitoring point was assessed using solid track detectors (*5*). Information regarding the physical conditions of the detector location, building structure, and other pertinent factors was documented, including the placement and collection dates. Monitoring spanned over 3 months, reflecting typical kindergarten operations. CR-39 was the track material in the solid track detectors, manufactured by the FUKUVI Chemical Company in Japan. Following collection, CR-39 chips were extracted, the etched using a 6.25 mol/L NaOH solution, and the track density was calculated by counting tracks under a microscope.

A dedicated database was established to store the gathered data, which was subsequently analyzed using SPSS (version 21.0; IBM, Armonk, US). Non-parametric tests were utilized to compare multiple sample means, with a significance level set at $P<0.05$.

RESULTS

Statistical analysis was performed on radon levels from 252 monitoring sites, revealing an average indoor radon concentration of 84.3 Bq/m^3 (Figure 1). Concentrations ranged from 12.9 to 263.5 Bq/m^3, with a median value of 76.8 Bq/m^3, detailed in Table 1. Figure 1 shows that 64.3% of sites had radon levels within the 50.0 to 100.0 Bq/m^3 range. Additionally, 13.1% reported levels below 50.0 Bq/m^3, and 20.2% had levels ranging from 100.0 to 200.0 Bq/m^3. Importantly, 2.4% of sites recorded radon concentrations exceeding 200.0 Bq/m^3.

The statistical analysis from Figure 2 indicated that indoor radon levels in 37 kindergartens across 18 administrative districts were all below the national standard limit of 300 Bq/m^3 (GB/T 16146-2015) (*6*). However, 7 kindergartens had radon concentrations exceeding 100 Bq/m^3. Notably, two kindergartens in Changping District had average indoor radon levels of 144.7 Bq/m^3 (median 155.7 Bq/m^3), significantly higher than other areas ($P<0.05$).

In our study, we analyzed the indoor radon concentrations in 37 kindergartens. A total of 108 surveillance points were placed on the first floor, 80 on the second floor, and 64 on the third floor or above.

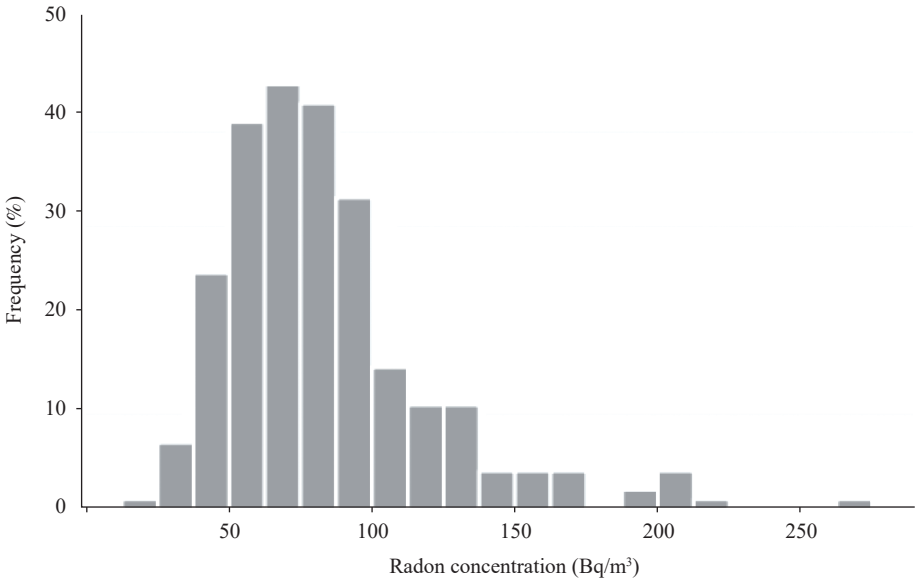

FIGURE 1. Frequency distribution of indoor radon concentration for 252 surveillance points.

TABLE 1. Results of indoor radon concentration for 252 surveillance points.

Descriptive index		Indoor radon concentration (Bq/m^3)
Average value		84.3
95% confidence interval for the mean	lower limit	79.7
	upper limit	88.9
Average values after 5% were pruned		80.9
Median		76.8
Variance		1,377.5
Standard deviation		37.1
Minimum value		12.9
Maximum value		263.5
Overall spread		250.6
Interquartile range		37.1
Skewness		1.6
Kurtosis		3.6

The monitoring results for each floor are shown in Figure 3.

On the first floor, indoor radon concentrations varied from 36.4 to 263.5 Bq/m^3, averaging 95.3 Bq/m^3 (median: 84.2 Bq/m^3). The second floor showed levels from 12.9 to 172.3 Bq/m^3, averaging 75.7 Bq/m^3 (median: 69.1 Bq/m^3). Radon concentrations for the third floor or higher ranged from 37.4 to 131.5 Bq/m^3, with an average of 76.3 Bq/m^3 (median: 75.1 Bq/m^3).

Our analysis reveals a significant discrepancy in indoor radon levels among various floors (P<0.05), with the highest concentration observed on the ground floor.

The mean indoor radon concentration in the children's area was 80.2 Bq/m^3 (median 75.1 Bq/m^3, range: 12.9–204.4 Bq/m^3). In the staff's area, the mean radon concentration was 92.5 Bq/m^3 (median 80.1 Bq/m^3, range: 34.1–263.5 Bq/m^3). Notably, six locations in kindergartens recorded radon levels exceeding 200.0 Bq/m^3 in 2023; these areas require continued monitoring in 2024. All 37 kindergartens monitored in this study were buildings constructed prior to 2016, highlighting a future need to enhance the surveillance and prevention efforts for kindergartens built after 2016 in accordance with new standards.

CONCLUSION

The current national standard GB/T 16146-2015 "Requirements for the Control of Indoor Radon and Its Progeny" (*6*) establishes specific indoor radon concentration limits for buildings constructed pre-2016 and post-2016: buildings constructed before 2016 should not exceed 300 Bq/m^3, and buildings constructed after January 1, 2016, should not exceed 100 Bq/m^3. However, the gradual decay of radon and its progeny, combined with factors like building materials and soil (*7*), challenges the effectiveness of these limits. The extended half-life of ^{226}Ra (1620 years) contributes to this issue (*8*), questioning the scientific foundation of the specified radon concentration thresholds for buildings pre-2016 and post-2016.

Children are more susceptible to radiation than adults (*9*). Prolonged exposure to indoor radon levels above 100 Bq/m^3 is a significant health concern, especially for children (*10*–*11*). It is crucial for governmental bodies, kindergartens, and health agencies to give priority to mitigating this issue. Specific guidelines for indoor radon limits tailored to children, accompanied by prevention and control measures, should be established in China. These actions will enhance the supervision, assessment, and prevention of indoor radon levels in kindergartens.

In this study, we evaluated indoor radon levels across 37 kindergartens in Beijing, uncovering that 18.9% had radon concentrations above the threshold of 100 Bq/m^3, deemed relatively high. Nonetheless, there is a notable absence of radon monitoring in kindergartens beyond Beijing. Given the variability in geological conditions, the ^{226}Ra levels in other regions could potentially exceed those in Beijing, presenting a significant health threat to children across China. Despite the existence of national guidelines for indoor radon prevention and control in buildings (GB/T 16146-2015), there are no tailored standards for kindergartens. Consequently, kindergartens tend to adhere to general building regulations, which may be insufficient. Notably, certain Beijing kindergartens exhibited radon levels reaching up to 263.5 Bq/m^3. This underscores the urgency of expanding radon surveillance in kindergartens throughout various provinces and cities, facilitating a science-based assessment that could prompt the formulation of dedicated standards to protect the health of young children.

Radon is an established carcinogen, specifically linked to lung cancer (*12*), yet its association with childhood leukemia remains under-acknowledged. Studies have confirmed radon's role in the etiology of

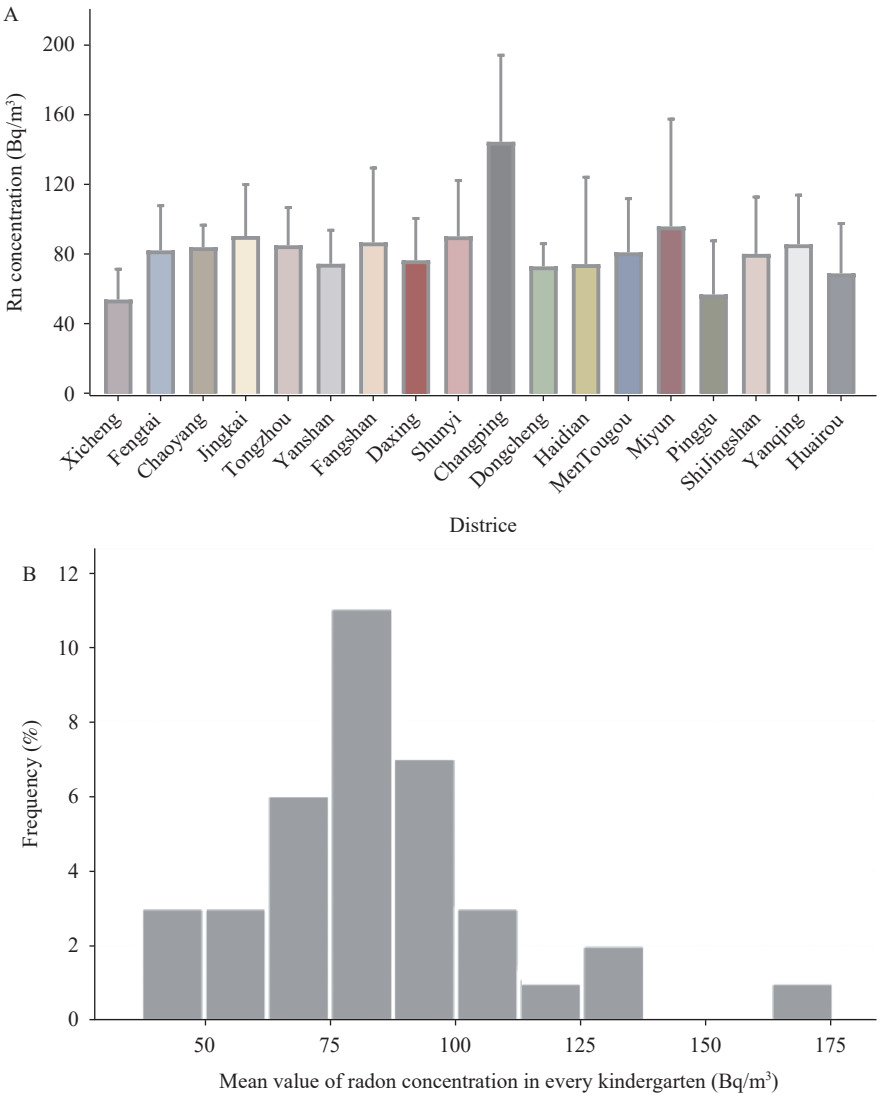

FIGURE 2. The indoor radon concentration situation of 37 kindergartens. (A) The average indoor radon concentration of kindergartens. (B) Frequency distribution of the mean radon concentration of 37 kindergartens.

leukemia (*10*). Observations indicate a heightened prevalence of childhood leukemia in certain regions of our country (*13*), prompting an investigation into the potential contribution of indoor radon to this pattern. Notably, children aged 2 to 6, who predominantly spend their time within kindergarten settings, are potentially at greater risk. It is essential to routinely assess radon levels in these environments to safeguard children's well-being during their pivotal developmental years. Research has demonstrated that radon concentrations are typically higher on lower floors of kindergartens, a factor closely associated with the properties of building materials and underlying soil (*14*). The structural designs of these establishments, often characterized by small windows, contribute to suboptimal ventilation, exacerbating radon accumulation. Moreover, children, by virtue of their shorter stature and proximity to the ground where radon concentrates, are exposed to greater levels of this gas compared with adults. Recognizing the significant health implications of indoor radon exposure for children, it is imperative to raise awareness, continually monitor radon levels in kindergartens, and establish rigorous radon control standards tailored for such institutions.

In conclusion, indoor radon concentrations in 37 kindergartens were found to be below the maximum limit of 300.0 Bq/m^3 as per the national standard GB/T 16146-2015 for building construction. However, 18.9% of the kindergartens exceeded the 100.0 Bq/m^3 limit specified for new buildings by the same standard. Currently, there is no specific indoor

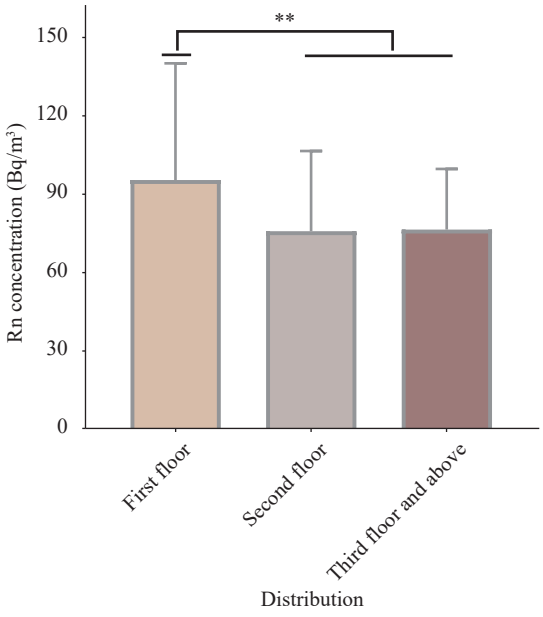

FIGURE 3. Distribution of indoor radon concentration across different floors.
** *P*<0.01.

radon control standard for kindergartens in China. It is recommended to enhance monitoring and establish a national standard to regulate indoor radon concentrations in kindergartens.

Conflicts of interest: No conflicts of interest.

Acknowledgements: Hongxing Cui and Bing Shang for their help with analysis and project guidance. CDCs in various districts (Xicheng, Fengtai, Chaoyang, Jingkai, Tongzhou, Yanshan, Fangshan, Daxing, Shunyi, Changping, Dongcheng, Haidian, Mentougou, Miyun, Pinggu, Shijingshan, Yanqing, and Huairou districts) for their assistance in determining detector locations.

Funding: Supported by the Construction Project of High-Level Public Health Technical Personnel in Beijing, China (Academic Leader-01-20).

doi: 10.46234/ccdcw2024.053

[#] Corresponding authors: Li Zhang, zhangli@chinacdc.cn; Yongzhong Ma, myz0905@126.com.

[1] Institute for Radiation Hygiene Protection, Beijing Center for Disease Prevention and Control, Beijing, China; [2] Chinese Center for Disease Control and Prevention, Beijing, China; [3] Key Laboratory of Radiological Protection and Nuclear Emergency & National Institute for Radiological Protection, Chinese Center for Disease Control and Prevention, Beijing, China.

Submitted: January 12, 2024; Accepted: February 26, 2024

REFERENCES

1. Choi H, Mazzone P. Radon and lung cancer: assessing and mitigating the risk. Cleve Clin J Med 2014;81(9):567 – 75. https://doi.org/10.3949/ccjm.81a.14046.
2. Blake TL, Chang AB, Marchant JM, McElrea MS. Respiratory health profile of Indigenous Australian children and young adults. J Paediatr Child Health 2020;56(7):1066 – 71. https://doi.org/10.1111/jpc.14817.
3. IARC Working Group on the Evaluation of Carcinogenic Risks to Humans. IARC monographs on the evaluation of carcinogenic risks to humans. Ingested nitrate and nitrite, and cyanobacterial peptide toxins. *IARC Monogr Eval Carcinog Risks Hum* 2010;94:v-vii, 1-412. https://pubmed.ncbi.nlm.nih.gov/21141240/.
4. Lecomte JF, Solomon S, Takala J, Jung T, Strand P, Murith C, et al. ICRP publication 126: radiological protection against radon exposure. Ann ICRP 2014;43(3):5 – 73. https://doi.org/10.1177/0146645314542212.
5. Vaupotič J, Smrekar N, Žunić ZS. Comparison of radon doses based on different radon monitoring approaches. J Environ Radioact 2017;169-170:19 – 26. https://doi.org/10.1016/j.jenvrad.2016.11.023.
6. General Administration of Quality Supervision, Inspection and Quarantine of the People's Republic of China, Standardization Administration of the People's Republic of China. GB/T 16146-2015 Requirements for control of indoor radon and its progeny. Beijing: Standards Press of China, 2016. http://www.csres.com/detail/269308.html. (In Chinese).
7. Stojanovska Z, Boev B, Zunic ZS, Ivanova K, Ristova M, Tsenova M, et al. Variation of indoor radon concentration and ambient dose equivalent rate in different outdoor and indoor environments. Radiat Environ Biophys 2016;55(2):171 – 83. https://doi.org/10.1007/s00411-016-0640-y.
8. Yarmoshenko IV, Malinovsky GP, Zhukovsky MV, Izgagin VS, Onishchenko AD, Vasilyev AV. Relationship between Ra-226 activity concentration in building materials and indoor radon concentration: an example of Russian high-rise residential buildings. J Environ Radioact 2024;272:107345. https://doi.org/10.1016/j.jenvrad.2023.107345.
9. Folkers C. Disproportionate impacts of radiation exposure on women, children, and pregnancy: taking back our narrative. J Hist Biol 2021;54(1):31 – 66. https://doi.org/10.1007/s10739-021-09630-z.
10. Moon J, Yoo H. Residential radon exposure and leukemia: a meta-analysis and dose-response meta-analyses for ecological, case-control, and cohort studies. Environ Res 2021;202:111714. https://doi.org/10.1016/j.envres.2021.111714.
11. Tong J, Qin LQ, Cao Y, Li JX, Zhang J, Nie JH, et al. Environmental radon exposure and childhood leukemia. J Toxicol Environ Health B Crit Rev 2012;15(5):332 – 47. https://doi.org/10.1080/10937404.2012.689555.
12. Mema SC, Baytalan G. Radon and lung cancer risk. CMAJ 2023;195(24):E850. https://doi.org/10.1503/cmaj.230110.
13. Ni X, Li Z, Li XP, Zhang X, Bai GL, Liu YY, et al. Socioeconomic inequalities in cancer incidence and access to health services among children and adolescents in China: a cross-sectional study. Lancet 2022;400(10357):1020 – 32. https://doi.org/10.1016/S0140-6736(22)01541-0.
14. Di Carlo C, Maiorana A, Ampollini M, Antignani S, Caprio M, Carpentieri C, et al. Models of radon exhalation from building structures: general and case-specific solutions. Sci Total Environ 2023;885:163800. https://doi.org/10.1016/j.scitotenv.2023.163800.

Youth Editorial Board

Indexed by Science Citation Index Expanded (SCIE), Social Sciences Citation Index (SSCI), PubMed Central (PMC), Scopus, Chinese Scientific and Technical Papers and Citations, and Chinese Science Citation Database (CSCD)

The inauguration of *China CDC Weekly* is in part supported by Project for Enhancing International Impact of China STM Journals Category D (PIIJ2-D-04-(2018)) of China Association for Science and Technology (CAST).

CCDC weekly

Vol. 6 No. 13 Mar. 29, 2024

Responsible Authority
National Disease Control and Prevention Administration

Sponsor
Chinese Center for Disease Control and Prevention

Editing and Publishing
China CDC Weekly Editorial Office
No.155 Changbai Road, Changping District, Beijing, China
Tel: 86-10-63150501, 63150701
Email: weekly@chinacdc.cn

CSSN
ISSN 2096-7071
CN 10-1629/R1